USGS
science for a changing world

Prepared in cooperation with Village of Ruidoso, New Mexico

# Geomorphic Survey of North Fork Eagle Creek, New Mexico, 2019

Open-File Report 2022–1041

U.S. Department of the Interior
U.S. Geological Survey

# Geomorphic Survey of North Fork Eagle Creek, New Mexico, 2019

By Alexander P. Graziano and Shaleene B. Chavarria

Prepared in cooperation with Village of Ruidoso, New Mexico

Open-File Report 2022–1041

**U.S. Department of the Interior**
**U.S. Geological Survey**

U.S. Geological Survey, Reston, Virginia: 2022

For more information on the USGS—the Federal source for science about the Earth, its natural and living resources, natural hazards, and the environment—visit https://www.usgs.gov or call 1–888–ASK–USGS.

For an overview of USGS information products, including maps, imagery, and publications, visit https://store.usgs.gov/.



Suggested citation:
Graziano, A.P., and Chavarria, S.B., 2022, Geomorphic survey of North Fork Eagle Creek, New Mexico, 2019: U.S. Geological Survey Open-File Report 2022–1041, 36 p., https://doi.org/10.3133/ofr20221041.

Associated data for this publication:
Graziano, A.P., and Chavarria, S.B., 2022, Data supporting the 2019 geomorphic survey of North Fork Eagle Creek, New Mexico: U.S. Geological Survey data release, https://doi.org/10.5066/P97ALYNZ.

U.S. Geological Survey, 2021, USGS water data for the Nation: U.S. Geological Survey National Water Information System database, https://doi.org/10.5066/F7P55KJN.

ISSN 2331-1258 (online)

# Contents



## Figures

## Tables

# Conversion Factors

U.S. customary units to International System of Units

| Multiply | By | To obtain |
|---|---|---|
| | Length | |
| foot (ft) | 0.3048 | meter (m) |
| mile (mi) | 1.609 | kilometer (km) |
| | Area | |
| acre | 4,047 | square meter ($m^2$) |
| acre | 0.4047 | hectare (ha) |
| acre | 0.4047 | square hectometer ($hm^2$) |
| acre | 0.004047 | square kilometer ($km^2$) |
| square foot ($ft^2$) | 929.0 | square centimeter ($cm^2$) |
| square foot ($ft^2$) | 0.09290 | square meter ($m^2$) |
| square mile ($mi^2$) | 259.0 | hectare (ha) |
| square mile ($mi^2$) | 2.590 | square kilometer ($km^2$) |
| | Flow rate | |
| cubic foot per second ($ft^3/s$) | 0.02832 | cubic meter per second ($m^3/s$) |
| | Hydraulic gradient | |
| foot per mile (ft/mi) | 0.1894 | meter per kilometer (m/km) |

# Datum

Vertical coordinate information is referenced to the North American Vertical Datum of 1988 (NAVD 88) or to the National Geodetic Vertical Datum of 1929 (NGVD 29), as indicated.

Horizontal coordinate information is referenced to the North American Datum of 1983 (NAD 83).

# Abbreviations

| | |
|---|---|
| LWD | large woody debris |
| RTK GNSS | real-time kinematic global navigation satellite system |
| SAC | slope-area computation |
| SACGUI | slope-area computation graphical user interface |
| USDA | U.S. Department of Agriculture |
| USGS | U.S. Geological Survey |

# Geomorphic Survey of North Fork Eagle Creek, New Mexico, 2019

By Alexander P. Graziano and Shaleene B. Chavarria

## Abstract

The 2012 Little Bear Fire resulted in substantial loss of vegetation in the Eagle Creek Basin, south-central New Mexico, which has been expected to cause a variety of hydrologic responses that could influence geomorphic change to North Fork Eagle Creek. To monitor geomorphic change, surveys of a downstream study reach of North Fork Eagle Creek were conducted in 2017, 2018, and 2019 by the U.S. Geological Survey in cooperation with the Village of Ruidoso, N. Mex. The study included surveys of select cross sections, woody debris accumulations, and pools found in the channel of the study reach. During 2017–19, high-flow events resulting from both monsoonal rainfall and snowmelt runoff occurred in the study reach, and the events appeared to have caused some minor localized geomorphic changes in the study reach, which were evaluated through comparison of the 2017, 2018, and 2019 survey results.

Comparisons of the cross-section survey results indicated that minor geomorphic changes had occurred in 4 of the 14 cross sections surveyed from 2017 to 2019. These geomorphic changes included aggradation or degradation of surface materials by about 1–2 feet in some parts of the affected cross sections. During the 2019 survey, 164 distinct accumulations of woody debris and 228 pools were identified in the study reach. Of the woody debris accumulations identified during the 2019 survey, 67 were certain to have also been present during the 2018 survey, and 21 were certain to have also been present during all three surveys (2017–19), indicating that most of the woody debris accumulations surveyed in 2017 were likely transported during the high-flow events between the 2017 and 2018 surveys. Most woody debris accumulations identified in 2019 did not appear to have substantially influenced geomorphic change in the locations where they were found but may have driven local geomorphic changes.

Because the study began 5 years after the 2012 Little Bear Fire and the geomorphic scope of the study has so far been limited, it cannot be said that the changes observed between the 2017 and 2019 surveys are representative of a pattern of geomorphic change following the Little Bear Fire. Once geomorphic changes identified during the 2017 through 2019 surveys can be compared with results from the remaining planned geomorphic surveys, it may be possible to develop an understanding of the patterns in geomorphic change following the 2012 Little Bear Fire.

## Introduction

Water supply for the Village of Ruidoso, New Mexico, is derived from surface-water and groundwater resources of the Eagle Creek and Rio Ruidoso Basins (U.S. Department of Agriculture [USDA] Forest Service, 2015), which are both located within the Upper Rio Hondo Basin in south-central New Mexico (fig. 1). On average, 24–29 percent of the annual water supply for the village is derived from three active (of four in total) production wells (hereafter referred to as "North Fork wells") located along North Fork Eagle Creek in the National Forest System lands of the Lincoln National Forest near Alto, N. Mex. (USDA Forest Service, 2016) (figs. 1 and 2). The North Fork Eagle Creek Basin is one of two basins (the other is the South Fork Eagle Creek Basin) that make up nearly all of the 8.14 square mile ($mi^2$) portion of the Eagle Creek Basin located upstream from the U.S. Geological Survey (USGS) Eagle Creek below South Fork near Alto, N. Mex., streamgage (USGS site 08387600; hereafter referred to as the "Eagle Creek streamgage") (fig. 2).

The North Fork wells began production in 1988, and the special use permit for operation of the wells (granted by the USDA Forest Service, Lincoln National Forest) expired in 1995 (USDA Forest Service, 2015). At that time, discussions began regarding the renewal of the special use permit (USDA Forest Service, 2015). A concern by some parties was the potential effect of well operations on streamflow in Eagle Creek (USDA Forest Service, 2015). As a result of these concerns, the USGS, in cooperation with the Village of Ruidoso, conducted a study of North Fork Eagle Creek from 2007 to 2009 to characterize the hydrology of the Eagle Creek Basin upstream from the Eagle Creek streamgage and the effects of groundwater pumping on streamflow (Matherne and others, 2010).

Following the USGS study (Matherne and others, 2010), the USDA Forest Service, Lincoln National Forest, issued the "North Fork Eagle Creek Wells Special Use Authorization Project Draft Environmental Impact Statement" in May

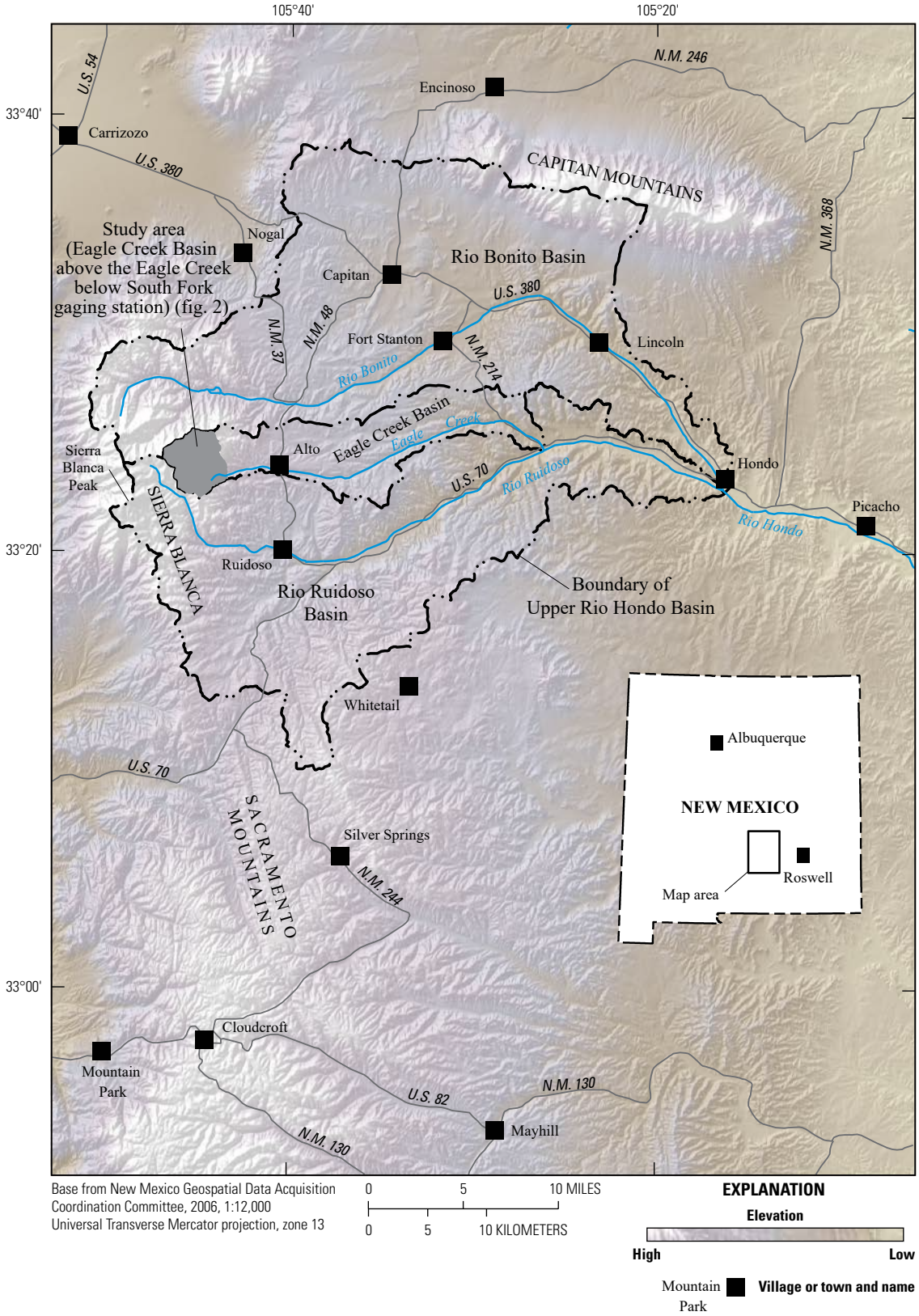


**Figure 1.** Location of the Eagle Creek Basin study area and geographic features in south-central New Mexico (modified from Matherne and others, 2010).

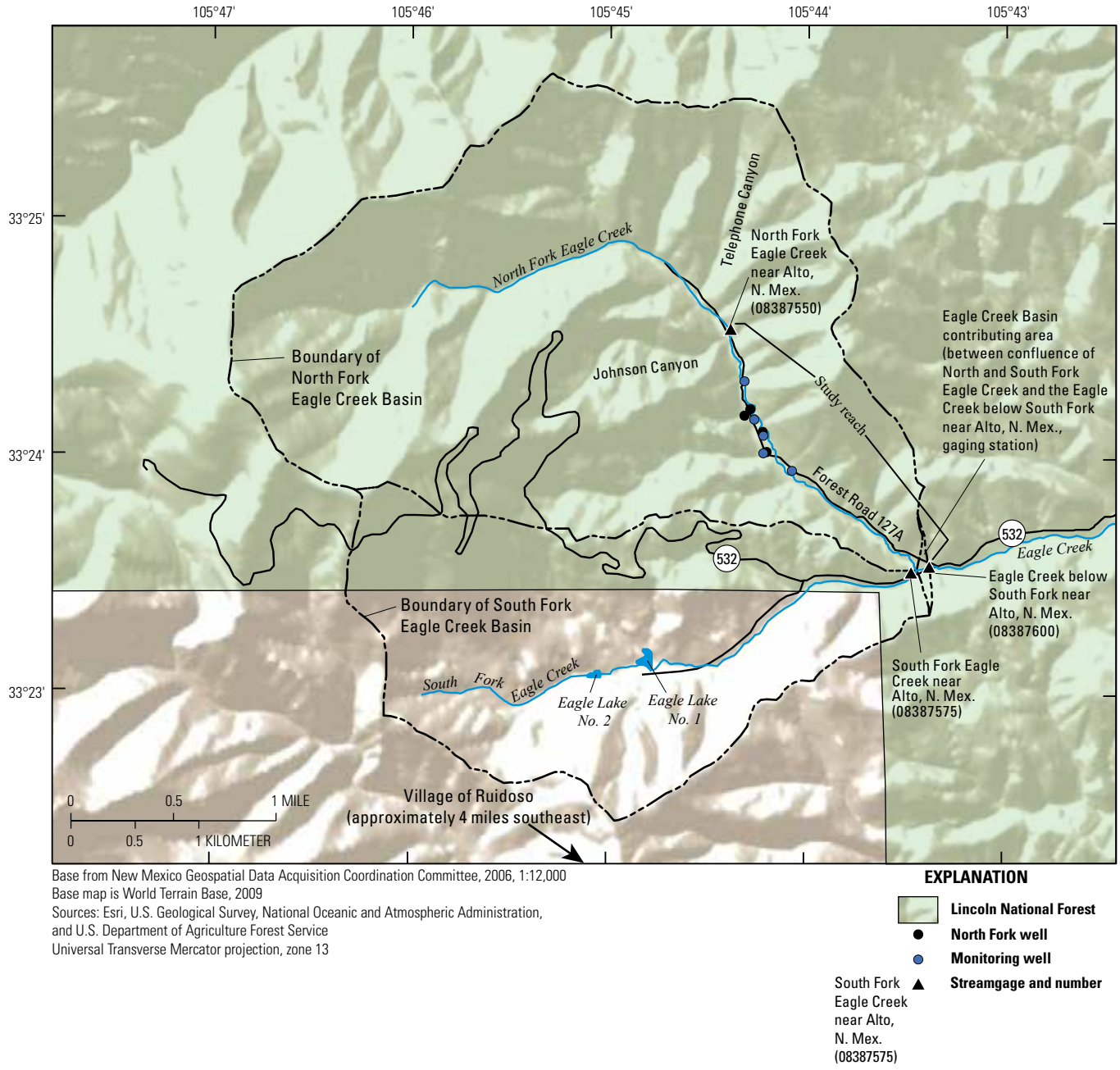


Base from New Mexico Geospatial Data Acquisition Coordination Committee, 2006, 1:12,000
Base map is World Terrain Base, 2009
Sources: Esri, U.S. Geological Survey, National Oceanic and Atmospheric Administration, and U.S. Department of Agriculture Forest Service
Universal Transverse Mercator projection, zone 13

**Figure 2.** Location of the study reach, North Fork and South Fork Eagle Creek Basins, Eagle Creek Basin contributing area, Lincoln National Forest boundaries, streamgages, and wells in the study area in the Eagle Creek Basin, south-central New Mexico (modified from Matherne and others, 2010).

2012, shortly before the start of the Little Bear Fire, which in June 2012 burned approximately 3,380 acres of the 3,400-acre North Fork Eagle Creek Basin (USDA Forest Service, 2015) (fig. 3). Burn severities in the basin ranged from high to very low or unburned. Specifically, 26 percent of the basin burned at high severity, 26 percent burned at moderate severity, 27 percent burned at low severity, and 21 percent either burned at very low severity or remained unburned (USDA Forest Service, 2015) (fig. 3). Notably, the North Fork Eagle Creek riparian corridor (defined as the area extending 200 feet [ft] on either side of the channel) primarily burned at low severity or less, and there was little loss of vegetation in this area (USDA Forest Service, 2015).

Following the Little Bear Fire, changes in some aspects of the hydrology of North Fork Eagle Creek were expected, including reduced infiltration and increased overland runoff, temporary increases in "flashy" responses to rainfall and snowmelt, increased sediment and debris yields, and changes to vegetation as a result of flooding (USDA Forest Service, 2016). On the basis of the altered postwildfire watershed

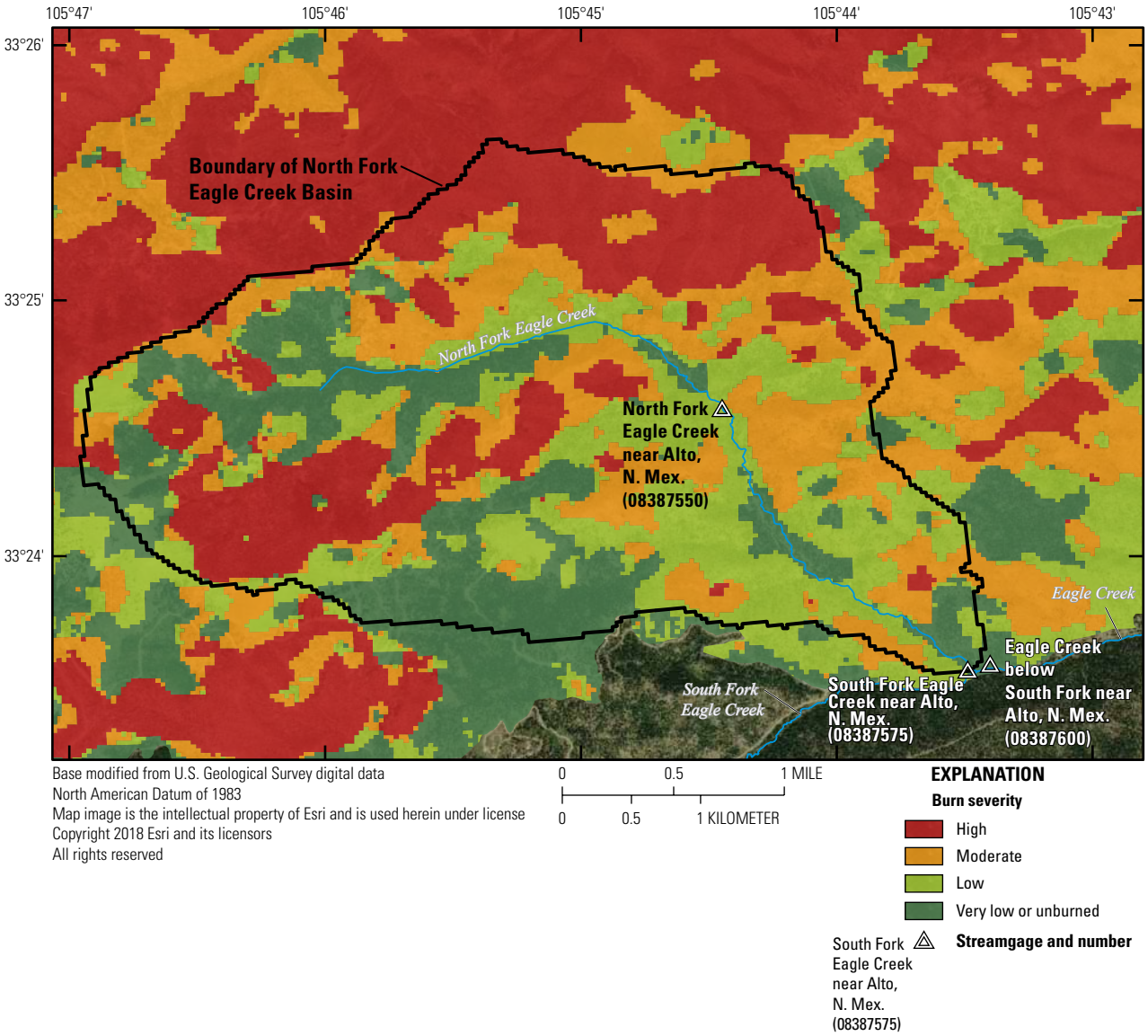


**Figure 3.** Little Bear Fire burn severity in the North Fork Eagle Creek Basin, south-central New Mexico, as established by the Burned Area Emergency Response (BAER) Team, June 18, 2012. Modified from data published in U.S. Department of Agriculture (USDA) Forest Service, Little Bear Fire BAER Team (2012).

conditions, a supplemental draft environmental impact statement was released by the USDA Forest Service, Lincoln National Forest, in 2014 (USDA Forest Service, 2015). In February 2016, the USDA Forest Service, Lincoln National Forest, released the "Record of Decision, North Fork Eagle Creek Wells Special Use Authorization," which established new monitoring and mitigation requirements but allowed the Village of Ruidoso to continue to operate the North Fork wells (USDA Forest Service, 2016).

The "Record of Decision, North Fork Eagle Creek Wells Special Use Authorization" established the one alternative, among those considered in the final environmental impact statement, that was to be implemented (USDA Forest Service, 2016). It also stipulated the terms and conditions of a new special use permit. Included in the decision were multiple monitoring measures designed to help determine direct or indirect effects of pumping on the quantity and quality of both surface water and groundwater. The Village of Ruidoso entered into a cooperative agreement with the USGS for assistance in one of these monitoring efforts, which involves periodic geomorphic surveys of a portion of North Fork Eagle Creek.

The objective of this study is to address the geomorphic monitoring requirements of the USDA Forest Service record of decision (USDA Forest Service, 2016) by conducting annual geomorphic surveys of North Fork Eagle Creek along the stream reach between the North Fork Eagle Creek near Alto, N. Mex., streamgage (USGS site 08387550; hereafter referred to as the "North Fork streamgage") and the Eagle

Creek streamgage (fig. 2). Specific plans for this study include conducting annual geomorphic surveys for 5 years (from 2017 to 2021), publishing all quality-assured survey data in a series of data releases, and publishing annual reports that summarize the surveyed geomorphic characteristics of the reach and changes from previous surveys.

## Purpose and Scope

The purpose of this report is to present the results from the 2019 geomorphic survey of North Fork Eagle Creek. The results from the 2019 geomorphic survey, which is the third of the five planned surveys, are summarized, interpreted, and compared to the results of the 2017 and 2018 surveys. The survey data used for this report are published in Graziano and Chavarria (2022), the companion data release of this report. In Graziano (2019), the results from the 2017 geomorphic survey are summarized and interpreted, and in Graziano (2020a), the results from the 2018 geomorphic survey are summarized, interpreted, and compared to the results of the 2017 survey. The survey data used for those reports are published in Graziano (2018) and Graziano (2020b), respectively.

## Study Area

The study area is the portion of the Eagle Creek Basin located upstream from the Eagle Creek streamgage (drainage area of 8.14 $mi^2$) (figs. 1 and 2; table 1). The study area is located on the eastern flank of the Sierra Blanca within the Upper Rio Hondo Basin, about 4 miles (mi) northwest of the Village of Ruidoso, N. Mex., and about 2.5 mi west of Alto, N. Mex. (fig. 1). Included in the study area are the North Fork Eagle Creek Basin (drainage area of 3.16 $mi^2$), the South Fork Eagle Creek Basin (drainage area of 2.79 $mi^2$), and a small contributing area from the Eagle Creek Basin (fig. 2). The study area is a forested mountain watershed where the dominant tree species are ponderosa pine (*Pinus ponderosa*) and mixed conifers (Matherne and others, 2010).

Streamflow in the study area is measured by the USGS at three streamgages (fig. 2; table 1). These streamgages include the previously mentioned North Fork and Eagle Creek streamgages in addition to the South Fork Eagle Creek near Alto, N. Mex., streamgage (USGS site 08387575; hereafter referred to as the "South Fork streamgage"). The Eagle Creek streamgage is located 270 ft (0.05 mi) downstream from the confluence of North Fork Eagle Creek and South Fork Eagle Creek, 1.84 mi downstream from the North Fork streamgage, and 430 ft (0.08 mi) downstream from the South Fork streamgage (fig. 2). The North Fork streamgage is located 1.79 mi upstream from the confluence of North Fork Eagle Creek and South Fork Eagle Creek, and the South Fork streamgage is located 160 ft (0.03 mi) upstream from the confluence of North Fork Eagle Creek and South Fork Eagle Creek (fig. 2).

The focus of the study is the North Fork Eagle Creek Basin, which was substantially burned by the 2012 Little Bear Fire (fig. 3). It is a mostly undeveloped basin, with exceptions including the wells and their associated infrastructure and a group of 22 cabins, which are mostly located upstream from the North Fork streamgage (Matherne and others, 2010). The basin is defined by narrow, steep drainages. The head of drainage for North Fork Eagle Creek has an elevation of about 10,500 ft above the North American Vertical Datum of 1988 (NAVD 88), whereas 4.5 mi downstream, the Eagle Creek streamgage (270 ft downstream from the mouth of North Fork Eagle Creek) has an elevation of about 7,600 ft above NAVD 88, giving North Fork Eagle Creek an average stream gradient of about 640 feet per mile (ft/mi) (Matherne and others, 2010).

The study reach begins about 260 ft upstream from the North Fork streamgage (where there is a bridge that carries Forest Road 127A over North Fork Eagle Creek) and ends at the Eagle Creek streamgage (fig. 2). In total, the study reach is 1.89 mi long. It is the same as the study reach defined for the 2018 survey (Graziano, 2020a), which is about 160 ft longer than the study reach defined for the 2017 survey (the study reach for the 2017 survey began about 100 ft upstream from the North Fork streamgage [Graziano, 2019] instead of 260 ft upstream from the North Fork streamgage).

Large sections of the study reach are characterized by intermittent streamflow, and streamflow volumes in the study reach have likely been affected by the North Fork wells that pump groundwater from the bedrock aquifer to supply water to the Village of Ruidoso (Matherne and others, 2010).

**Table 1.** U.S. Geological Survey streamgages in the North Fork Eagle Creek Basin study area in the Eagle Creek Basin, south-central New Mexico.

[Locations shown in figure 2; data from U.S. Geological Survey, 2021a, b, c; $mi^2$, square mile; NGVD 29, National Geodetic Vertical Datum of 1929; N. Mex., New Mexico]

| Site name | Site number | Period of record | Drainage area ($mi^2$) | Elevation (feet above NGVD 29) |
|---|---|---|---|---|
| Eagle Creek below South Fork near Alto, N. Mex. | 08387600 | 1969–80; 1988–present | 8.14 | 7,600 |
| North Fork Eagle Creek near Alto, N. Mex. | 08387550 | 2007–present | 3.16 | 7,900 |
| South Fork Eagle Creek near Alto, N. Mex. | 08387575 | 2007–present | 2.79 | 7,630 |

Specifically, Matherne and others (2010) estimated that, for an 11-year period before the North Fork wells were drilled (from 1970 to 1980), groundwater flow out of the basin represented about 33 percent of basin yield and that, for a 13-year period after the North Fork wells were put into service (from 1988 to 2000), groundwater flow out of the basin represented about 16 percent of basin yield and mean annual groundwater pumping represented about 17 percent of basin yield. Additionally, Matherne and others (2010) approximated that, beginning about 1,600 ft (0.3 mi) downstream from the North Fork streamgage, the streambed has the capacity to transmit water into the bedrock aquifer at a rate of about 0.7–1 cubic foot per second ($ft^3/s$); therefore, if it is assumed that the bedrock aquifer would be saturated if groundwater pumping had never occurred, then water being transmitted to the aquifer would instead be flowing continuously or saturating the alluvium. However, Matherne and others (2010) concluded that streamflow in some part of the stream channel between the North Fork and Eagle Creek streamgages was likely intermittent during parts of both a 10-year period before the North Fork wells were drilled (from 1970 to 1979) and a 20-year period after they were drilled (from 1989 to 2008) on the basis of alluvium and channel configurations and the available streamflow records.

Matherne and others (2010) also found that the sum of streamflows recorded at the South Fork and North Fork streamgages was greater than the streamflow recorded at the Eagle Creek streamgage at most times during the 19-month period from September 2007 through March 2009. If streamflow were not lost to aquifer or alluvium infiltration in the reach of North Fork Eagle Creek located below the North Fork streamgage, then it would be expected that the sum of the streamflows recorded at the South Fork and North Fork streamgages would always be less than or equal to the streamflow at the Eagle Creek streamgage.

# Methods

The field survey was conducted during June 17–20, 2019, when continuous streamflow (recorded at 15-minute intervals) at the North Fork streamgage ranged from 0.14 to 0.27 $ft^3/s$ (U.S. Geological Survey, 2021b), continuous streamflow at the Eagle Creek streamgage ranged from 0.13 to 0.24 $ft^3/s$ (U.S. Geological Survey, 2021a), and a total of about 1 mi of the 1.89 mi study reach was observed to be dry at the surface at the time it was surveyed. During the 2019 field survey, the 14 cross-section locations established in 2017 (Graziano, 2019) (fig. 4) were resurveyed by using USGS techniques and methods for single-base real-time kinematic global navigation satellite system (RTK GNSS) surveys (Rydlund and Densmore, 2012). All accumulations of woody debris, all pools, and all other features of geomorphic significance found in the reach were identified, cataloged, photographed, and surveyed for location (by using RTK GNSS receivers or estimation methods). All accumulations of woody debris were classified by their potential to form debris jams, all pools were measured for residual depth, and select pools were surveyed for thalweg elevation by using RTK GNSS receivers.

## Cross-Section Surveys

In 2017, cross sections were surveyed at 14 locations along the study reach on North Fork Eagle Creek (Graziano, 2019) (fig. 4). The cross-section locations were initially chosen on the basis of equal distance estimations, with one cross section established approximately every 1,500 ft, beginning 100 ft upstream from the North Fork streamgage and ending 380 ft upstream from the confluence with South Fork Eagle Creek (Graziano, 2019). Additional cross sections were then established in 2017 at locations that were thought to be particularly susceptible to geomorphic change. These additional cross sections were established directly downstream from tributaries and road crossings and in the middle of large flood deposits (which were identified as sections of the study reach where floodplain vegetation was sparse and floodplain surface materials were primarily composed of coarse, unconsolidated sediments that appeared to have been transported and deposited during recent seasonal high-flow events).

At the 14 locations where cross sections were established and surveyed in 2017, reference marks for future surveys were monumented in concrete on both banks (Graziano, 2019). In 2019, those reference marks were used to identify and resurvey the same 14 cross sections (fig. 4). Cross sections were surveyed from the left to the right from the perspective oriented downstream and included points within the channel and on the adjacent floodplains. Cross sections were surveyed in accordance with USGS standard protocols (Benson and Dalrymple, 1967), whereby individual surveyed points were selected on the basis of where substantial changes in slope occurred. Selected survey points also included the points of lowest elevation in each cross section.

Individual cross-section points were surveyed for location and elevation by using USGS techniques and methods for single-base RTK GNSS surveys as described in Rydlund and Densmore (2012). The Online Positioning User Service (OPUS; National Geodetic Survey, 2020) was used with one base station position to correct all cross-section points to the North American Datum of 1983 (NAD 83) and NAVD 88. Horizontal and vertical positional accuracies for most points ranged from plus or minus (±) 0.1 to ±0.3 ft, relative to those datums. In Graziano and Chavarria (2022), all cross-section points with positional accuracies poorer than ±0.3 ft are noted.

## Cross-Section Plots and Characteristics

Cross-section plots were developed by using the slope-area computation graphical user interface (SACGUI) application (Bradley, 2012). SACGUI utilizes version 7 of the

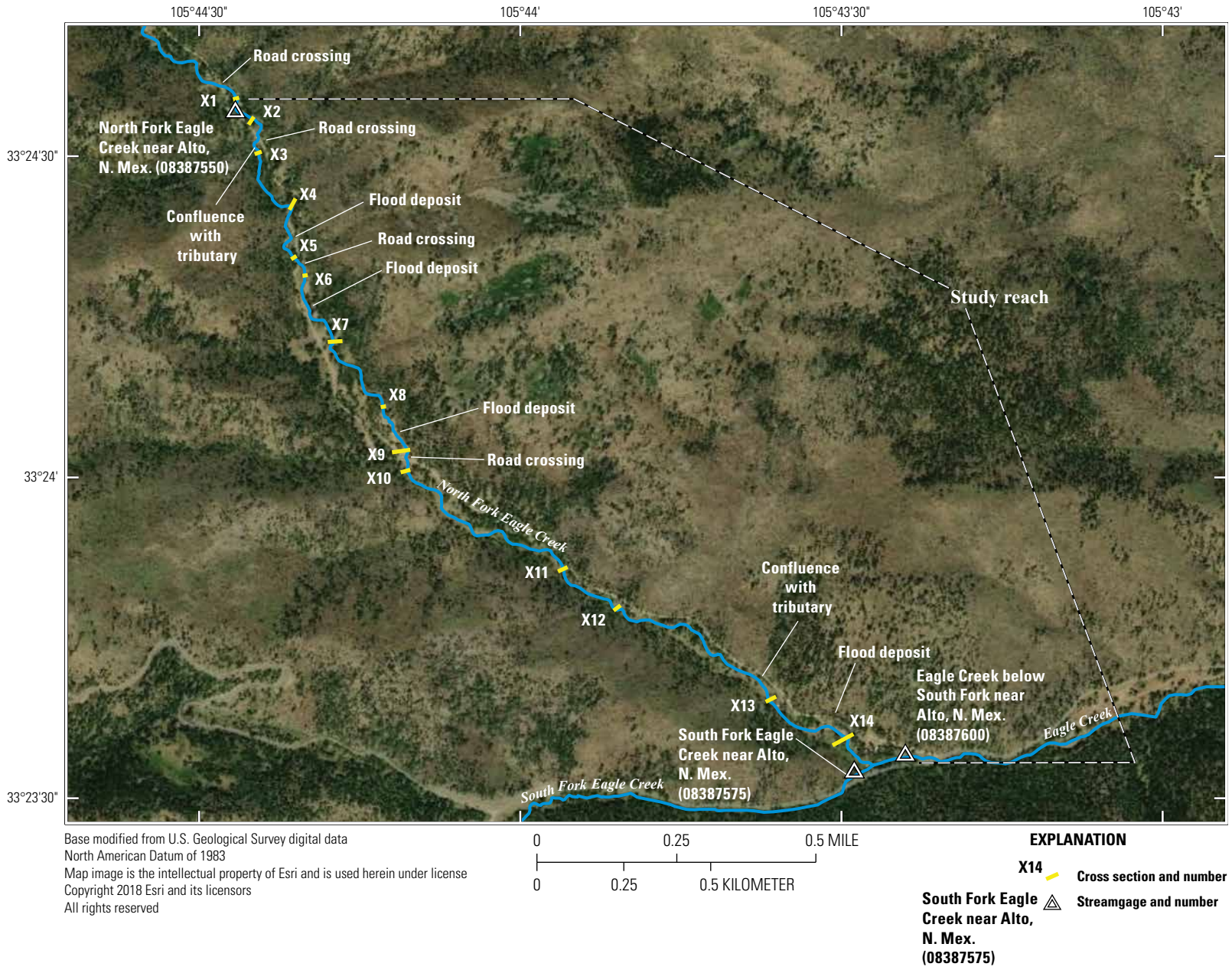


**Figure 4.** Study reach with locations of streamgages, locations and extents of cross sections, and locations of other features in the North Fork Eagle Creek Basin, south-central New Mexico, 2019.

slope-area computation (SAC) program, which is described in Fulford (1994). SAC was developed on the basis of the standard USGS slope-area measurement technique presented in Dalrymple and Benson (1968). SACGUI includes a method for the development of cross-section plots by using x-y-z coordinates. For this study, SACGUI was used to convert x-y coordinates to "distance from left bank" values, which represent the distance from the left bank reference mark. Additionally, on the basis of bankfull stage estimates, other cross-section characteristics (including channel width and area and bank height and slope) either were calculated in SACGUI or were derived from SACGUI output files.

Bankfull stage is the water level of the bankfull discharge, which has been defined as the streamflow that completely fills the channel without spilling onto the floodplain (Leopold and others, 1964; Knighton, 1998). Estimates of bankfull stage were largely based on field observations of bank locations but were also informed by the cross-section plots, the photographs of the cross sections, and the bankfull stage estimates that were made for the 2017 and 2018 surveys (Graziano, 2019, 2020a). The primary topographic features used to determine bankfull stage were the abrupt decreases in slope typically associated with the transition between the channel and the floodplain. These determinations were then secondarily verified by changes in terrain and vegetation. However, because the point at which there was a transition between the channel and the floodplain was poorly defined in some areas, making good estimates of bankfull stage was difficult for some cross-section locations. Additionally, determination of bankfull stage is characteristically subjective (Johnson and Heil, 1996). Therefore, to retain consistency in the methods used to determine bankfull stage, two criteria established in Graziano (2019) for the 2018 survey were adapted for estimating bankfull stage for the 2019 survey of North Fork Eagle Creek.

First, because the tops of the left and right banks were never at the exact same height but were often close enough in height that either could be reasonably used for estimating bankfull stage, it was decided that estimates of bankfull stage would always be based directly on the lower height of the two banks. Second, at the locations where banks were well defined, the channel often appeared to be between 1 and 3 ft deep; therefore, it was decided that for the locations where banks were poorly defined any decreases in slope between the depths of about 1 and 3 ft would be carefully considered when making estimates of bankfull stage. In Graziano (2019, p. 9), a third criterion established for making estimates of bankfull stage stated, "if it was found that the initial choice for bankfull stage was at a stage which could hypothetically result in water flowing or pooling in a smaller side channel, then to reduce uncertainty in channel characteristic determinations, bankfull stage was lowered to a stage just below the base of the smaller side channel, where, at that stage, it could be assumed that flow would only be occurring in the main channel." This criterion was not followed when bankfull stage was estimated during the 2018 or 2019 surveys because there were some well-defined banks of the main channel that were at elevations above the deepest points of the side channels, and using this criterion would result in inaccurate estimates of bankfull stage in those areas. Where these side channels were present, the cross-section characteristics discussed in the next paragraph were calculated on the basis of the main channel alone.

Estimates of bankfull stage were then used to calculate the following characteristics for each cross section: maximum depth at bankfull stage (in feet), cross-section width (in feet), cross-section area (in square feet), left and right bank heights (in feet), and left and right bank slopes (dimensionless, in feet per foot). Maximum depth at bankfull stage was defined as the depth of the thalweg at bankfull stage. Cross-section width was defined as the width of the water surface of the main channel at bankfull stage. Cross-section area was defined as the wetted area of the main channel at bankfull stage. Left and right bank heights were defined as the heights of the two banks of the main channel at bankfull stage, and left and right bank slopes were defined as the slopes of the two banks of the main channel at bankfull stage. Maximum depths, cross-section areas, and cross-section widths at bankfull stage were calculated in SACGUI. Bank heights and slopes were calculated on the basis of field observations and interpretations of SACGUI results. Specifically, bank heights and slopes were calculated by defining top of bank as the point at which bankfull stage intersected with the left or right bank and by defining bottom of bank as the cross-section point at the base of the corresponding left or right bank. Cross-section points that represented the bases of banks were primarily identified in the field and were typically found to be points at the edges of the channel where abrupt increases in slope began.

## Woody Debris

Woody debris is an important component of forested watersheds that can substantially affect the hydrology, geomorphology, and ecology of streams (Wallace and others, 1995; Abbe and Montgomery, 1996; Gurnell and others, 2002). Geomorphic studies of woody debris often focus on large woody debris (LWD), typically defined as logs and branches greater than 0.3 ft in diameter and 5 ft in length (Heimann, 2017), a definition that is also used for LWD in this report. Importantly, LWD can serve as "key members" in debris jams (Abbe and Montgomery, 1996), meaning that they can initiate the formation of debris jams. Debris jams can control pool and bar formation (Abbe and Montgomery, 1996), pool spacing (Montgomery and others, 1995), and sediment storage, channel width, and stream gradient (Nakamura and Swanson, 1993), in addition to other geomorphic channel characteristics (Gurnell and others, 2002).

During the 2019 survey, all areas where woody debris accumulated in the channel of the study reach on North Fork Eagle Creek were identified, cataloged, photographed, and surveyed for location (using the same methods that were used for the 2018 survey [Graziano, 2020a] and generally the same

methods that were used for the 2017 survey [Graziano, 2019] but with more rigorous application). Woody debris was identified by walking the study reach of the channel from upstream to downstream. Generally, areas with woody debris of any size were cataloged and referred to as "woody debris accumulations," including individually scattered pieces of LWD and small piles of twigs and sticks. However, individually scattered twigs and sticks were not cataloged, photographed, or surveyed for location, as this type of debris mostly looked to have fallen directly into the channel from nearby trees instead of being deposited by streamflow. Additionally, the potential geomorphic effects of this type of debris were presumed to be insignificant.

Woody debris accumulations were surveyed for location mostly by using the same RTK GNSS methods that were used to survey the cross-section points. However, many woody debris accumulations were found in places where RTK GNSS reception was poor; therefore, the locations of most woody debris accumulations determined by using RTK GNSS receivers have approximate horizontal positional accuracies ranging from ±0.1 to ±3.0 ft relative to NAD 83. In Graziano and Chavarria (2022), all woody debris accumulations with horizontal positional accuracies poorer than ±3.0 ft (that were surveyed by using RTK GNSS) are noted. Additionally, because of various considerations (such as RTK GNSS reception issues), the precise points surveyed for woody debris accumulations were not consistent (that is, some woody debris accumulations were surveyed near their centers, and others were surveyed closer to one of their edges). For woody debris accumulations where location was not determined by using RTK GNSS receivers, the locations were estimated by using field notes (which included estimated distances between all features), photographs, and digital mapping software (specifically, Google Earth [Alphabet Inc., Mountain View, California]). The horizontal positional accuracies of locations determined by using this method were estimated to be ±50 ft. This accuracy estimate was largely based on how well the estimated distances between features surveyed using RTK GNSS (from the field notes) compared with the actual distances between those features (from the RTK GNSS survey results). In Graziano and Chavarria (2022), the location source (either RTK GNSS or digital map) is included for each surveyed point.

From the photographs, all identified woody debris accumulations were later classified on the basis of whether they were debris deposits, potential debris jams, or active debris jams. These classifications were originally defined in Graziano (2019) for the 2017 survey. For the 2019 survey (as well as the 2018 survey), the definitions remained the same and are given in the next three paragraphs (with some modifications to their wordings).

Debris deposits are defined as areas containing pieces of woody debris that appear to have been deposited in a largely random fashion on the recessions of wood-mobilizing streamflows (Graziano, 2019). Debris deposits could be found anywhere in the channel and could include scattered LWD or loose accumulations of smaller woody debris. Because debris deposits were not characterized by debris packed together tightly and did not appear to contain key members that could potentially initiate the formation of a debris jam (particularly, not in the location where they were found), they were not identified as active or potential debris jams (which are defined in the next two paragraphs). Further, the LWD of debris deposits often did not meet the size limit for LWD (0.3 ft in diameter and 5 ft long), and they did not typically retain any branches; therefore, the likelihood that this type of debris could later snag, or anchor, and thereby become a key member of a debris jam was presumed to be low. Pieces from debris deposits could, however, later add to the volume of debris jams downstream.

Potential debris jams are defined as areas containing pieces of LWD that have the potential to later serve as key members in debris jams (Graziano, 2019). The LWD found in potential debris jams could be trees that fell from the adjacent floodplain or hillslope into or across the channel (and may still be anchored to the bank), logs that were placed across the channel by people (for recreational purposes), or logs that were carried downstream by high flows (and settled perpendicular or oblique to flow direction and were long enough to span most, if not all, of the channel in their settled locations). The likelihood that the LWD found in these areas could become key members in debris jams, particularly in the areas where they were found, was presumed to be higher than that of the woody debris accumulations defined as debris deposits.

Active debris jams are defined as areas where debris jams have already formed (Graziano, 2019). They were identified by the presence of woody debris and possibly other debris (including grass, pine cones, pine needles, and sediment) packed tightly against one or more key members of woody debris. Further, the tightly packed debris was usually observed to be on the upstream side of the key members. The key members were typically LWD, but because of the relatively small size of the channel in some locations, they could be smaller than the LWD definition used for this study. Because woody debris jams can control geomorphic channel characteristics, active debris jams were presumed to be the most likely woody debris accumulations that had served or could later serve as drivers of geomorphic change in the study reach.

## Pools

Pools, which are important components of stream ecosystems, provide habitat for various aquatic species (Wallace and others, 1995) and contribute to hydraulic complexity, which supports habitat diversity (Buffington and others, 2002). Pool dimensions and frequency can be affected by woody debris (Montgomery and others, 1995; Abbe and Montgomery, 1996), sediment load (Madej and Ozaki, 1996), and other watershed disturbances (Lisle, 1982).

During the 2019 survey, all pools in the main channel of the study reach on North Fork Eagle Creek were identified, cataloged, photographed, surveyed for location, and measured for residual depth. Additionally, the deepest parts of select pools (where RTK GNSS reception was good) were surveyed for thalweg elevation. In wet sections of the study reach, pools were identified as locations at base flow where velocities decreased and water depths increased. They were verified by the presence of downstream riffle crests or artificial weirs, which were at higher elevations than the channel thalweg and controlled the stage. In dry sections of the study reach, pools were primarily identified as locations where the thalweg of the channel appeared to be longitudinally concave and, in the presence of water, would presumably adopt the features previously mentioned.

Pools were surveyed for location by using the same methods that were used for the woody debris accumulations. The locations of pools determined by using RTK GNSS receivers have approximate horizontal positional accuracies ranging from ±0.1 to ±3.0 ft relative to NAD 83. In Graziano and Chavarria (2022), all pools with horizontal positional accuracies poorer than ±3.0 ft (that were surveyed by using RTK GNSS) are noted. Additionally, because of various considerations (such as RTK GNSS reception issues), the precise points surveyed for pools were mostly inconsistent (that is, some pools were surveyed at the location of their deepest point, but others were surveyed closer to one of their edges). The locations of pools determined by using field notes, photographs, and digital mapping software have horizontal positional accuracies estimated to be ±50 ft. Like with the woody debris accumulations, this accuracy estimate was largely based on how well the estimated distances between features surveyed by using RTK GNSS (from the field notes) compared with the actual distances between those features (from the RTK GNSS survey results). For the select pools where thalweg elevations were also surveyed and published, the approximate local horizontal and vertical positional accuracies range from ±0.1 to ±0.3 ft, relative to NAD 83 and NAVD 88. In Graziano and Chavarria (2022), the location source (either RTK GNSS or digital map) is included for each surveyed point.

During the 2019 survey, pools were measured for residual depth (these measurements were also made during the 2018 survey but were not made during the 2017 survey). Residual depth is the difference in depth or bed elevation between a pool and the downstream riffle crest (Lisle, 1987). Residual depth is a simple, unbiased, and ecologically important pool dimension that is independent of variations caused by streamflow (Lisle, 1987) and is therefore a good metric for monitoring geomorphic change to pools over time.

For measuring residual depth at pools identified in wet sections of the study reach, an engineer's rule was used to measure water depth at both the deepest part of each pool and the deepest part of each pool's downstream riffle crest. Residual depth for each pool was calculated by taking the difference between the two values. Using this method, residual depths were measured to the nearest 0.01 ft, and on the basis of uncertainty in the correct selection of the deepest parts of the pools and riffle crests, accuracy was estimated to be ±0.1 ft.

For measuring residual depth at pools identified in dry sections of the study reach, a survey rod with engineer's scale was held vertically at the deepest part of each dry pool, and the depth of the lowest point of each dry pool's downstream riffle crest was roughly measured by line of sight. The depth determined for each dry pool's downstream riffle crest was the residual depth. Using this method, the residual depths were measured to the nearest 0.5 ft, and the accuracy was estimated to be ±0.5 ft, which means that dry pools with residual depths of 0.5 ft were within the level of detection but may not actually function as pools during periods when water is present. The large uncertainty in the residual depths of dry pools reflects the difficulty in both the identification of pools and the measuring of the residual depths of pools in dry sections of the study reach. Graziano and Chavarria (2022) includes information on the streamflow condition (flowing, standing, or dry) for each pool at the time it was surveyed.

On the basis of the residual depth results from the 2018 survey and of the accuracy of the dry pool measurements, residual depth classifications were developed for all pools surveyed in 2018 (Graziano 2020a). All pools with residual depths less than 0.75 ft were classified as shallow, all pools with residual depths between 0.75 and 1.25 ft were classified as intermediate, and all pools with residual depths greater than 1.25 ft were classified as deep. These same classifications are used in this report.

## Other Features of Geomorphic Significance

Beginning with the 2018 survey and continuing with the 2019 survey, other features of geomorphic significance (including road crossings, flood deposits, tributary confluences, channel bifurcations, and fine-sediment accumulations) found in the study reach on North Fork Eagle Creek were identified, cataloged, photographed, and surveyed for location. Road crossings were identified as locations where the study reach crosses Forest Road 127A (fig. 2) by flowing under a bridge or through a culvert or as locations where the study reach crosses Forest Road 127A by flowing over it (that is, locations where vehicles on Forest Road 127A are required to ford the stream channel to cross it). Flood deposits were identified as sections of the study reach where floodplain vegetation was sparse and floodplain surface materials were primarily composed of coarse, unconsolidated sediments that appeared to have been transported and deposited during recent seasonal high-flow events. The larger flood deposits were also associated with braiding of the channel. Tributary confluences were identified either by flowing water seen entering the study reach during the survey or by the presence of culverts seen along the road adjacent to the study reach. Channel bifurcations were identified as areas where the main

channel forked before reconverging again within about 100 ft (for each channel bifurcation, points both where the channel forked and where the channel reconverged were identified and surveyed). Areas where the channel appeared to separate into more than two distributaries were not identified as channel bifurcations. Fine-sediment accumulations were identified as fine-grained deposits (finer than those in the surrounding streambed) that were impounded by obstructions in the main channel (for example, woody debris accumulations, boulders, and bedrock).

Notably, the methods for identifying fine-sediment accumulations were not rigorously adhered to during the 2019 survey (or the 2018 survey); therefore, the catalog of these features was not comprehensive for the study reach. However, because at least some fine-sediment accumulations were photographed and surveyed, the information that was collected for them can be used for spot monitoring of geomorphic change to the study reach. For example, the photographs taken of these features during the 2019 and 2018 surveys and those planned to be taken during future surveys may provide evidence of qualitative changes. If the fine-sediment accumulations or other identifiable features (such as the colocated active debris jams) remain in place, the photographs taken during the 2019 and 2018 surveys and those planned to be taken during future surveys may provide evidence of change, either to the stability or the dimensions of the fine-sediment accumulations.

Road crossings and flood deposits were first identified in the field during the 2018 survey and then located by using aerial imagery from March 2016 in Google Earth. These features were identified again in the same locations during the 2019 survey. Because the locations of road crossings and flood deposits were defined as points (rather than polygons) and could be verified by characteristics that were visible in aerial imagery (for example, in aerial imagery, flood deposits could be identified by a lack of vegetation and by sand-colored surface material extending out 25 ft or more from the sides of the channel), horizontal positional accuracy for those features was not determined because it would not have exceeded the relatively large size of the features. For the rest of the features of geomorphic significance, the locations were determined by using either RTK GNSS receivers or the estimation methods used for woody debris accumulations and pools. Therefore, the locations of other features of geomorphic significance that were determined by using RTK GNSS receivers have approximate horizontal positional accuracies ranging from ±0.1 to ±3.0 ft relative to NAD 83. The locations of other features of geomorphic significance that were determined by using field notes, photographs, and digital mapping software have estimated horizontal positional accuracies of ±50 ft. In Graziano and Chavarria (2022), the location source (either RTK GNSS or digital map) is included for each surveyed point.

## Considerations in the Comparison of the 2017, 2018, and 2019 Survey Results

To compare the results of the 2017, 2018, and 2019 geomorphic surveys of North Fork Eagle Creek, certain discrepancies among the three datasets needed to be considered and accounted for. First, all of the published cross-section elevation data from the 2017 and 2018 surveys (Graziano, 2018, 2020b) needed to be corrected to NAVD 88 (the vertical datum of the 2019 survey). The cross-section elevation data published for the 2017 and 2018 surveys had mostly good quality local vertical positional accuracies (±0.1 to ±0.2 ft) and were surveyed in NAVD 88, but the vertical positional accuracies relative to NAVD 88 were unknown at the time that the 2017 and 2018 survey data were published (Graziano, 2019, 2020a). The 2019 survey cross-section data, on the other hand, had mostly good quality vertical positional accuracies (±0.1 to ±0.3 ft) locally and relative to NAVD 88. Therefore, the elevations of select cross-section reference marks from 2019 were used to correct all cross-section elevation data from 2017 and 2018 for comparison and plotting purposes. Specifically, the 2017 elevation data for cross sections 1 through 10 were corrected by adding 2.60 ft (this calculated factor was based on the difference between the elevation surveyed for the right bank reference mark at cross section 3 in 2017 and 2019), and the 2017 elevation data for cross sections 11 through 14 were corrected by adding 0.38 ft (this calculated factor was based on the difference between the elevation surveyed for the left bank reference mark at cross section 13 in 2017 and 2019). The 2018 elevation data for cross sections 1 through 6 were corrected by adding 7.80 ft (this calculated factor was based on the difference between the elevation surveyed for the right bank reference mark at cross section 3 in 2018 and 2019), the 2018 elevation data for cross sections 7 through 10 were corrected by adding 8.43 ft (this calculated factor was based on the difference between the elevation surveyed for the right bank reference mark at cross section 8 in 2018 and 2019), and the 2018 elevation data for cross sections 11 through 14 were corrected by adding 8.47 ft (this calculated factor was based on the difference between the elevation surveyed for the left bank reference mark at cross section 13 in 2018 and 2019). Single correction factors for each year could not be used because the base station was moved during both the 2017 and 2018 surveys. These corrections introduced about ±0.1 to ±0.2 ft of additional uncertainty to the comparisons.

Second, the 2019 distance published in Graziano and Chavarria (2022) for cross section 4 needed to be corrected to be accurately compared with the 2017 and 2018 surveys of cross section 4. This correction was necessary because the horizontal positions of three of the points in cross section 4 in 2019 were surveyed with poor accuracy (greater than 3.3 ft). The 2019 distances for cross section 4 were corrected by adding 10.63 ft (this calculated factor was based on the difference between the right bank reference mark distance from 2019 and the average distance of the right bank reference marks from 2017 and 2018).

Third, other sources of uncertainty in cross-section data comparisons included the RTK GNSS accuracies (discussed in the "Cross-Section Surveys" section) and the roughness of the topography. Features that contributed to the roughness of the topography included coarse surface materials, such as rocks and vegetation. Field measurements that could be used to calculate uncertainty from the roughness of the topography have not been made; therefore, uncertainties in 2017, 2018, and 2019 cross-section data comparisons could not be completely and accurately quantified. However, these sources of uncertainty were considered and are discussed in the comparison of the channel-profile and cross-section results from the 2017, 2018, and 2019 surveys in the "Geomorphic Survey of North Fork Eagle Creek in 2019" section.

Other discrepancies that were considered when comparing the results of the 2018 and 2019 surveys to the 2017 survey included possible differences in the methods used for identifying woody debris accumulations and known differences in the methods used for identifying pools. These discrepancies were also sources of uncertainty that were considered and are discussed where woody debris accumulation and pool survey results from 2018 and 2019 are compared to the results from the 2017 survey. Generally, photographic evidence was heavily relied on for these comparisons.

# Streamflow in the Period Between the 2017 and 2019 Surveys

In this section, the streamflow records that are presented and discussed are primarily those for the period between the 2017 and 2019 geomorphic surveys. Streamflow records from before the 2017 geomorphic survey were presented and discussed in Graziano (2019). Generally, Graziano (2019) found that, for the period up to 2017 (see table 1 for the period of record for individual streamgages), streamflow at the streamgages in the Eagle Creek Basin most often remained less than 2.00 $ft^3/s$. Sustained periods of streamflow greater than 2.00 $ft^3/s$ were typically a result of snowmelt runoff in March, April, and May. It was approximated by Matherne and others (2010) that sustained streamflow greater than 2.20 $ft^3/s$ is needed to maintain continuous streamflow in North Fork Eagle Creek. Graziano (2019) also found that, for the period ending in 2017, peak annual streamflows greater than 50.00 $ft^3/s$ had about a 2-year recurrence interval at both the North Fork and Eagle Creek streamgages. At all three streamgages in the Eagle Creek Basin, when peak annual streamflows greater than 50.00 $ft^3/s$ occurred, they were most often a result of heavy rainfall occurring during the North American monsoon season of July through September.

## June 19, 2017, to June 14, 2018

For the time period starting on the last day of the 2017 survey and ending on the last day of the 2018 survey (June 19, 2017, to June 14, 2018; Graziano, 2020a), daily mean streamflow at the Eagle Creek streamgage (fig. 2) was less than 2.00 $ft^3/s$ for 325 of the 361 days (U.S. Geological Survey, 2021a). There were two distinct high-flow events during which peak instantaneous streamflow exceeded 50.00 $ft^3/s$ at the Eagle Creek streamgage during the period from June 19, 2017, to June 14, 2018. The two high-flow events had peak instantaneous streamflows of 98.50 and 118.00 $ft^3/s$, which occurred on July 31, 2017, and February 16, 2018, respectively (U.S. Geological Survey, 2021a).

At the North Fork streamgage, daily mean streamflow ranged from 0.13 $ft^3/s$, which occurred on June 12, 2018, and June 13, 2018, to 40.30 $ft^3/s$, which occurred on February 17, 2018 (the same day as the maximum daily mean streamflow at the Eagle Creek streamgage for the period from June 19, 2017, to June 14, 2018) (U.S. Geological Survey, 2021a, b). Daily mean streamflow at the North Fork streamgage was less than 2.00 $ft^3/s$ for 332 of the 361 days from June 19, 2017, to June 14, 2018 (U.S. Geological Survey, 2021b).

Daily mean streamflow at the South Fork streamgage for the period from June 19, 2017, to June 14, 2018, ranged from 0.08 $ft^3/s$, which occurred on May 31, 2018, and June 1, 2018, to 1.47 $ft^3/s$, which occurred on July 31, 2017 (the same day as one of the peak instantaneous streamflows greater than 50.00 $ft^3/s$ at the Eagle Creek streamgage for the period from June 19, 2017, to June 14, 2018) (U.S. Geological Survey, 2021a, c). Daily mean streamflows at the South Fork streamgage were less than 1.00 $ft^3/s$ for 346 of the 361 days from June 19, 2017, to June 14, 2018 (U.S. Geological Survey, 2021c).

## June 14, 2018, to June 20, 2019

Daily mean streamflow at the Eagle Creek streamgage for the period starting on the last day of the 2018 survey and ending on the last day of the 2019 survey (June 14, 2018, to June 20, 2019) ranged from 0.00 $ft^3/s$, which occurred from June 14, 2018, to June 16, 2018, to 84.20 $ft^3/s$, which occurred on October 24, 2018 (U.S. Geological Survey, 2021a) (fig. 5*A*). Daily mean streamflows were less than 2.00 $ft^3/s$ for 208 of the 372 days from June 14, 2018, to June 20, 2019 (U.S. Geological Survey, 2021a) (fig. 5*A*). Since USGS gaging at this location first began in 1969, daily mean streamflow has mostly remained less than 2.00 $ft^3/s$ (Graziano, 2019).

There were two distinct high-flow events during which peak instantaneous streamflow exceeded 50.00 $ft^3/s$ at the Eagle Creek streamgage during the period from June 14, 2018, to June 20, 2019. The two high-flow events had peak instantaneous streamflows of 140.00 and 59.40 $ft^3/s$, which occurred on October 24, 2018, and January 6, 2019, respectively (U.S. Geological Survey, 2021a) (fig. 5*A*). The high-flow event that

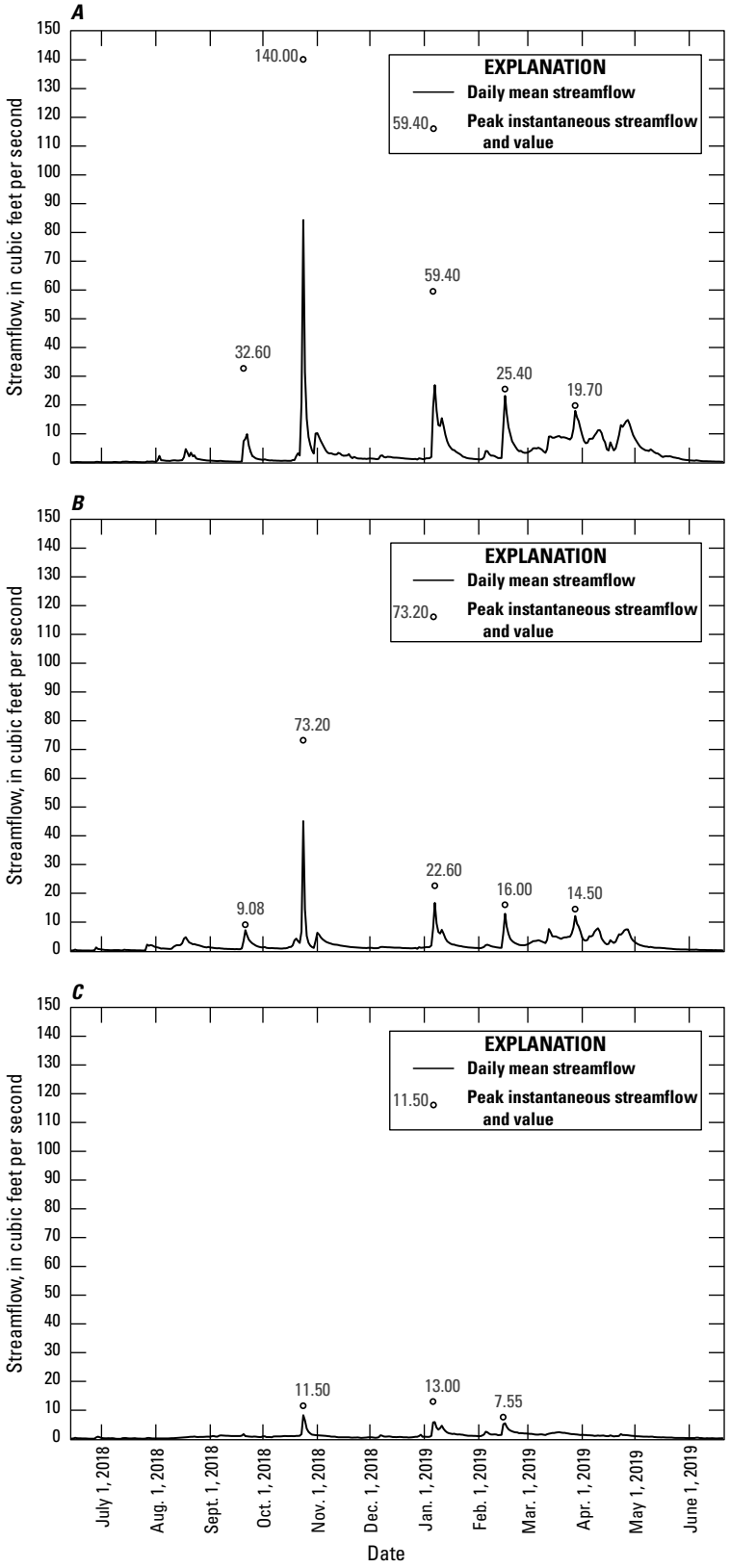


**Figure 5.** Daily mean streamflow and select peak instantaneous streamflow at the three streamgages in the Eagle Creek Basin, south-central New Mexico, June 14, 2018, to June 20, 2019. *A*, Eagle Creek below South Fork near Alto, N. Mex., streamgage (U.S. Geological Survey [USGS] site 08387600) (U.S. Geological Survey, 2021a). *B*, North Fork Eagle Creek near Alto, N. Mex., streamgage (USGS site 08387550) (U.S. Geological Survey, 2021b). *C*, South Fork Eagle Creek near Alto, N. Mex., streamgage (USGS site 08387575) (U.S. Geological Survey, 2021c).

produced the peak on October 24, 2018, was less flashy than the high-flow event that produced the peak on January 6, 2019. The peak on October 24, 2018, was preceded by a peak flow of 111.00 $ft^3/s$ that occurred 9 hours after the start of the event, at which time streamflow slightly receded, and was followed by a secondary peak of 140.00 $ft^3/s$ 18 hours after the start of the event (or 9 hours after the first peak of 111.00 $ft^3/s$). The event on January 6, 2019, was flashier than the October 24, 2018, event and reached peak streamflow 9 hours after the start of the event. Streamflow during this event remained greater than 50.00 $ft^3/s$ for 30 minutes, whereas streamflow during the October 24, 2018, event remained greater than 50.00 $ft^3/s$ for 11 hours (U.S. Geological Survey, 2021a).

Daily mean streamflow at the North Fork streamgage for the period from June 14, 2018, to June 20, 2019, ranged from 0.10 $ft^3/s$, which occurred on June 25, 2018, to 45.10 $ft^3/s$, which occurred on October 24, 2018 (the same day as the maximum daily mean streamflow at the Eagle Creek streamgage for the period from June 14, 2018, to June 20, 2019) (U.S. Geological Survey, 2021a, b) (fig. 5*A* and *B*). Daily mean streamflows at the North Fork streamgage were less than 2.00 $ft^3/s$ for 238 of the 372 days from June 14, 2018, to June 20, 2019 (U.S. Geological Survey, 2021b) (fig. 5*B*). Since USGS gaging at this location first began in 2007, daily mean streamflow has mostly remained less than 2.00 $ft^3/s$ (Graziano, 2019), which means that streamflow between the North Fork and Eagle Creek streamgages has likely been discontinuous for a majority of the time since 2007 (based on the approximation in Matherne and others [2010] that sustained streamflows greater than 2.20 $ft^3/s$ are needed to maintain continuous streamflow in North Fork Eagle Creek).

There was only one distinct high-flow event in which peak instantaneous streamflow exceeded 50.00 $ft^3/s$ at the North Fork streamgage during the period from June 14, 2018, to June 20, 2019. The high-flow event had a peak instantaneous streamflow of 73.20 $ft^3/s$, which occurred on October 24, 2018 (U.S. Geological Survey, 2021b) (fig. 5*B*). Like the peak at the Eagle Creek streamgage, the peak at the North Fork streamgage on October 24, 2018, was not reached until about 14 hours after the high-flow event began (U.S. Geological Survey, 2021a, b). However, unlike the streamflow during the event that produced the peak at the Eagle Creek streamgage on October 24, 2018, which remained greater than 50.00 $ft^3/s$ for about 11 hours in total, the streamflow during the event that produced the peak at the North Fork streamgage on October 24, 2018, remained greater than 50.00 $ft^3/s$ for only about 5 hours in total (U.S. Geological Survey, 2021a, b).

Daily mean streamflow at the South Fork streamgage for the period from June 14, 2018, to June 20, 2019, ranged from 0.03 $ft^3/s$, which occurred on June 12, 2018, and June 1, 2018, to 8.23 $ft^3/s$, which occurred on October 24, 2018 (the same day as one of the peak instantaneous streamflows greater than 50.00 $ft^3/s$ at the Eagle Creek streamgage and the peak instantaneous streamflow at the North Fork streamgage for the period from June 14, 2018, to June 20, 2019) (U.S. Geological Survey, 2021a, b, c) (fig. 5). Daily mean streamflows at the South Fork streamgage were less than 1.00 $ft^3/s$ for 221 of the 372 days from June 14, 2018, to June 20, 2019 (U.S. Geological Survey, 2021c) (fig. 5*C*). Since USGS gaging at this location first began in 2007, daily mean streamflow has mostly remained less than 1.00 $ft^3/s$ (Graziano, 2019). There were no high-flow events in which peak instantaneous streamflow exceeded 50.00 $ft^3/s$ at the South Fork streamgage during the period from June 14, 2018, to June 20, 2019 (U.S. Geological Survey, 2021c) (fig. 5*C*).

For 244 of the 372 days from June 14, 2018, to June 20, 2019, the sums of the daily mean streamflows recorded at the North Fork and South Fork streamgages were higher than the daily mean streamflow recorded at the Eagle Creek streamgage (U.S. Geological Survey, 2021a, b, c), and streamflows at the streamgages were at their typical levels (less than 2.00 $ft^3/s$ at the Eagle Creek and North Fork streamgages and less than 1.00 $ft^3/s$ at the South Fork streamgage). The higher combined streamflows from the North Fork and South Fork streamgages are evidence that, during the 244 days, substantial portions of the water flowing by the North Fork streamgage were likely being lost to aquifer recharge or alluvium saturation in the reach of North Fork Eagle Creek located below the North Fork streamgage. For the other 128 of the 372 days from June 14, 2018, to June 20, 2019, the sums of the daily mean streamflows recorded at the North Fork and South Fork streamgages were lower than the daily mean streamflow recorded at the Eagle Creek streamgage (U.S. Geological Survey, 2021a, b, c).

## Geomorphic Survey of North Fork Eagle Creek in 2019

The results of the 2019 geomorphic survey, presented in the following sections, have been derived from field notes, field photographs, and the companion data release (Graziano and Chavarria, 2022). The data release contains the full set of survey points and includes their unique identifiers, locations (as horizontal coordinates), elevations (for cross-section points and the deepest points of select pools), "distance from left bank" values (for cross-section points), classifications (for woody debris accumulations), residual depths (for pools), descriptions, and location sources. Also included are indications of whether water was present or absent at each point at the time it was surveyed. The results of the 2017 and 2018 geomorphic surveys, which are compared to the results of the 2019 geomorphic survey in the following sections, are published in Graziano (2019, 2020a). Because of the horizontal and vertical datum differences discussed in the "Methods" section, the 2017 and 2018 survey results were modified for this report where the channel-profile and cross-section results of those two previous surveys are compared.

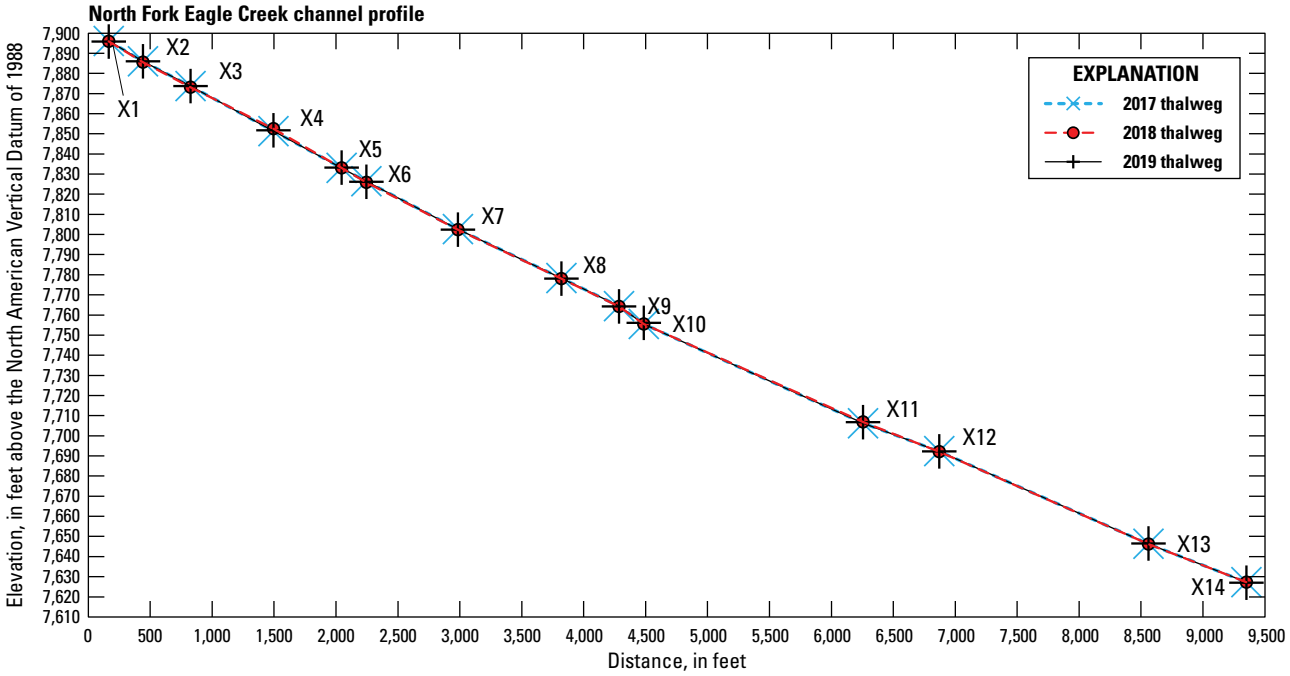


**Figure 6.** Channel profile from cross section 1 (X1) to cross section 14 (X14) of the study reach on North Fork Eagle Creek, Eagle Creek Basin, south-central New Mexico, 2017, 2018, and 2019. Elevations from 2017 and 2018 have been corrected to the 2019 vertical datum on the basis of the differences among the 2017, 2018, and 2019 cross-section reference mark elevations.

**Table 2.** Channel profile data from cross sections of the study reach on North Fork Eagle Creek, Eagle Creek Basin, south-central New Mexico, 2017 through 2019.

[Distances are based on the study reach trace in figure 4 and are rounded to the nearest 5 feet; 2017 and 2018 elevation data have been corrected to the 2019 vertical datum on the basis of the differences among the 2017, 2018, and 2019 cross-section reference mark elevations; stream gradients were calculated on a cross-section to cross-section basis and were assigned to the upstream cross section (for example, the stream gradient assigned to cross section 1 is for the river reach between cross sections 1 and 2); ft, foot; NAVD 88, North American Vertical Datum of 1988; ft/mi, foot per mile, –, not applicable]

| Cross-section number | Distance downstream (ft) | 2017 thalweg elevation (ft above NAVD 88) | 2017 stream gradient (ft/mi) | 2018 thalweg elevation (ft above NAVD 88) | 2018 stream gradient (ft/mi) | 2019 thalweg elevation (ft above NAVD 88) | 2019 stream gradient (ft/mi) |
|---|---|---|---|---|---|---|---|
| 1 | 165 | 7,896.1 | 194 | 7,896.0 | 200 | 7,895.8 | 188 |
| 2 | 440 | 7,886.0 | 169 | 7,885.6 | 171 | 7,886.0 | 169 |
| 3 | 825 | 7,873.7 | 177 | 7,873.1 | 162 | 7,873.7 | 173 |
| 4 | 1,495 | 7,851.3 | 176 | 7,852.6 | 187 | 7,851.7 | 178 |
| 5 | 2,045 | 7,833.0 | 174 | 7,833.1 | 190 | 7,833.2 | 187 |
| 6 | 2,245 | 7,826.4 | 170 | 7,825.9 | 168 | 7,826.1 | 169 |
| 7 | 2,985 | 7,802.6 | 154 | 7,802.4 | 154 | 7,802.4 | 154 |
| 8 | 3,820 | 7,778.3 | 158 | 7,778.0 | 157 | 7,778.1 | 158 |
| 9 | 4,285 | 7,764.4 | 235 | 7,764.2 | 230 | 7,764.2 | 214 |
| 10 | 4,485 | 7,755.5 | 147 | 7,755.5 | 145 | 7,756.1 | 147 |
| 11 | 6,255 | 7,706.2 | 119 | 7,706.9 | 127 | 7,706.7 | 124 |
| 12 | 6,870 | 7,692.3 | 144 | 7,692.1 | 143 | 7,692.2 | 143 |
| 13 | 8,560 | 7,646.3 | 127 | 7,646.2 | 127 | 7,646.5 | 130 |
| 14 | 9,350 | 7,627.3 | – | 7,627.2 | – | 7,627.0 | – |

## Channel Profile

A channel profile of the study reach, from cross section 1 to cross section 14, was developed on the basis of the cross-section thalweg points surveyed in 2019. The new 2019 channel profile was compared to the channel profile of the study reach from the 2017 and 2018 surveys (fig. 6; table 2). The 2019 survey results demonstrate that between cross section 1 and cross section 14 there was 268.8 ft of fall over 9,185 ft (1.74 mi), which computes to an average gradient of about 164 ft/mi for the study reach. Using the 2017 and 2018 cross-section elevation data that have been corrected to the 2019 vertical datum, the average gradient for the study reach in 2017 and 2018 was calculated to be about 165 ft/mi and 166 ft/mi, respectively.

Calculations of stream gradient along the thalweg from cross section to cross section from the 2019 survey yield results that range from 124 ft/mi, for the reach segment between cross sections 11 and 12, to 214 ft/mi, for the reach segment between cross sections 9 and 10 (table 2). The gradients for all other cross-section-defined reach segments were between 130 and 188 ft/mi.

In comparison to 2019, calculations of stream gradient from cross section to cross section from the 2018 survey yield results that range from 127 ft/mi, for the reach segment between cross sections 11 and 12 (and cross sections 13 and 14), to 230 ft/mi, for the reach segment between cross sections 9 and 10. Calculations of stream gradient from the 2017 survey yield results that range from 119 ft/mi, for the reach segment between cross sections 11 and 12, to 235 ft/mi, for the reach segment between cross sections 9 and 10. Excluding the two end extremes (maximum and minimum), the gradients for all other cross-section-defined reach segments from 2018 were between 143 and 200 ft/mi, and those from 2017 were between 127 and 194 ft/mi. The cross sections with lower gradients measured during the 2017, 2018, and 2019 surveys tended to remain relatively stable over the years, unlike the cross sections with steeper gradients, where there was a maximum change of 16 ft/mi between the 2017 and 2018 surveys at cross section 5 and a maximum change of 16 ft/mi between the 2018 and 2019 surveys at cross section 9. However, these differences among the stream gradient results from 2017 to 2019 may be more attributable to the coarseness of the channel bed material at the thalweg and the limited accuracies of the survey readings than to actual physical changes to the stream gradient.

## Cross-Section Plots and Characteristics

Cross-section plots for the 2017, 2018, and 2019 surveys (fig. 7) (created from the cross-section data published in the Graziano [2018, 2020b] and Graziano and Chavarria [2022] data releases) and cross-section characteristics from the 2017 (Graziano, 2019), 2018 (Graziano, 2020a), and 2019 (table 3) surveys indicated that channel geometries throughout the study reach varied among the three surveys. In 2019, maximum depth at bankfull stage ranged from 1.4 to 6.8 ft, cross-section channel width ranged from 10.7 to 54.6 ft, cross-section channel area ranged from 12.8 to 90.0 square feet ($ft^2$), bank heights ranged from 0.8 to 6.0 ft, and bank slopes ranged from 0.1 to 0.8 (dimensionless, in feet per foot) (table 3).

In 2018, maximum depth at bankfull stage ranged from 1.5 to 7.5 ft, cross-section channel width ranged from 13.6 to 94.4 ft, cross-section channel area ranged from 15.8 to 225.0 $ft^2$, bank heights ranged from 0.7 to 7.2 ft, and bank slopes ranged from 0.1 to 2.2 (dimensionless, in feet per foot) (Graziano, 2020a). Notably, the maximum values in cross-section channel width, cross-section channel area, and left bank height differed from the 2019 maximum values. The discrepancies in the maximum values between 2018 and 2019 survey data are due to poor quality survey points in cross sections 4, 8, 10, 11, and 14. These were the cross sections where maximums were observed in the 2018 survey data but where 2019 values could not be calculated (table 3) because of poor quality survey points. As noted in Graziano (2020b), many of the cross-section characteristics from the 2018 survey are not directly comparable to the ranges for the cross-section characteristics from the 2017 survey because for cross sections 2, 3, 8, 9, 11, 12, and 14 the bankfull stages were largely redefined for the 2018 survey, primarily on the basis of better quality bank observations rather than physical changes to the cross sections. Therefore, instead of comparing cross-section characteristics derived from bankfull stage to evaluate changes to the cross sections from 2017 to 2019, the cross-section plots were directly compared (fig. 7).

Comparisons of the cross-section plots, as well as references to field and aerial photographs, from 2017 through 2019 indicated that cross sections 3, 7, and 10 were the three most likely cross sections to have undergone topographic changes caused by fluvial processes (fig. 7*C*, *G*, and *J*). For all other cross sections, topographic changes were difficult to discern because the changes seen in the cross-section plots were likely more attributable to the roughness of the topography and vegetative growth on the banks of the channel and in the channel and to the poor quality of the survey points than to physical changes to the cross-section topographies. For example, the roughness of the topography was likely the largest source of change for cross sections 4, 9, 13, and 14 either because there was a fair amount of vegetation in the channel or because the channel bed at those cross sections was partially composed of boulders (some of which were greater than 1 ft in diameter and could affect the placement of the survey rod, thereby ultimately impacting survey data) (fig. 7*D*, *I*, *M*, and *N*). The poor quality of the survey readings was likely the largest source of change for cross sections 1 and 8 because there was about 3.5 ft of uncertainty in the horizontal datum correction used to compare the 2017 and 2018 plots of cross section 1 (fig. 7*A*) and about 1.1 ft of uncertainty in the vertical datum correction used to compare the 2017 and 2018 plots of cross section 8 (fig. 7*H*).

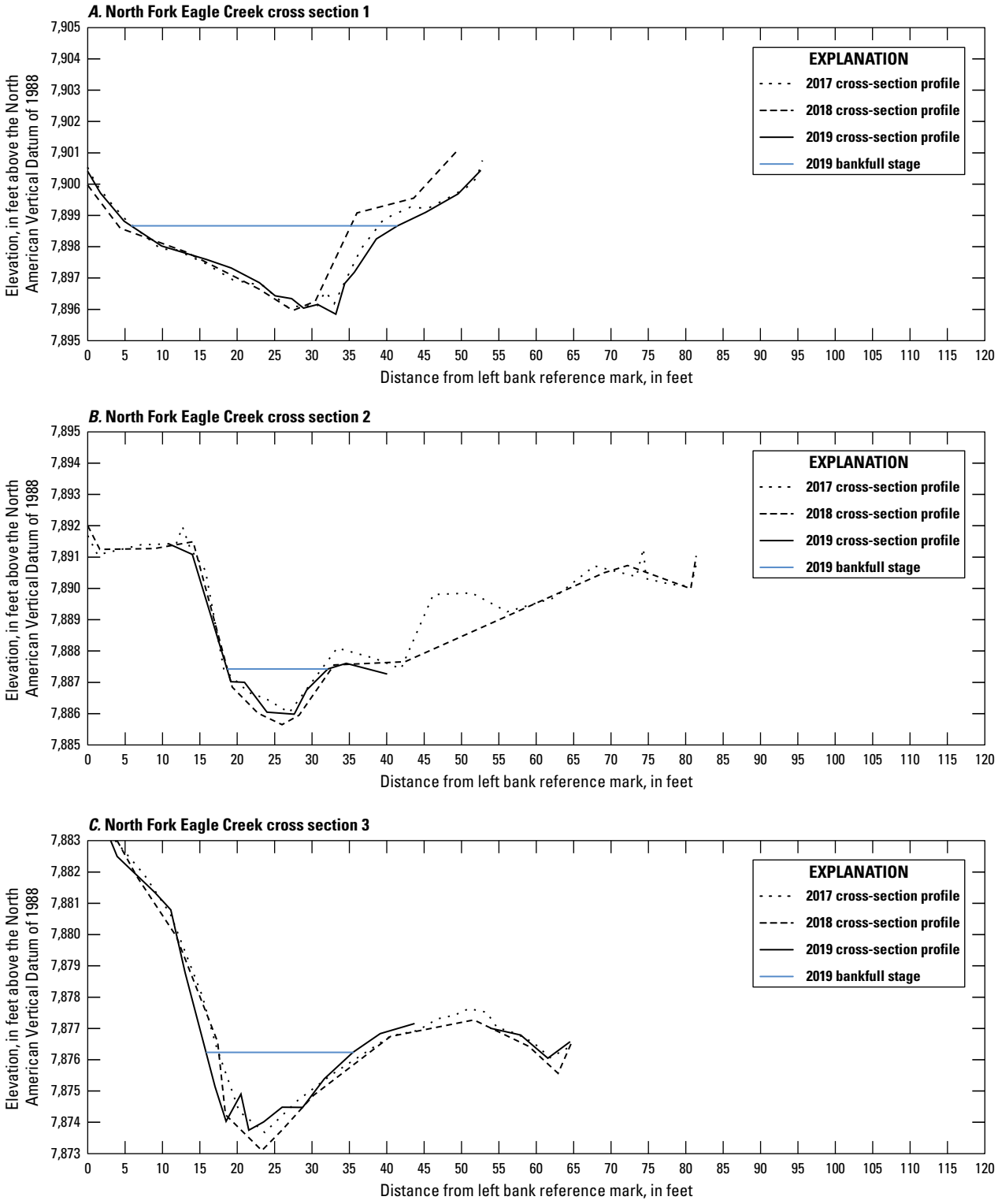


**Figure 7.** Channel cross section 1 to cross section 14 (in downstream order) from the 2017, 2018, and 2019 surveys plotted with 2019 estimates of bankfull stage for the study reach on North Fork Eagle Creek, Eagle Creek Basin, south-central New Mexico. Distances and elevations from 2017 and 2018 have been corrected to the 2019 horizontal and vertical datums on the basis of the differences among the 2017, 2018, and 2019 cross-section reference mark locations and elevations. Areas where there are breaks in the cross-section plots indicate poor quality survey data that were disqualified for use. *A*, Cross section 1. *B*, Cross section 2. *C*, Cross section 3. *D*, Cross section 4. *E*, Cross section 5. *F*, Cross section 6. *G*, Cross section 7. *H*, Cross section 8. *I*, Cross section 9. *J*, Cross section 10. *K*, Cross section 11. *L*, Cross section 12. *M*, Cross section 13. *N*, Cross section 14.

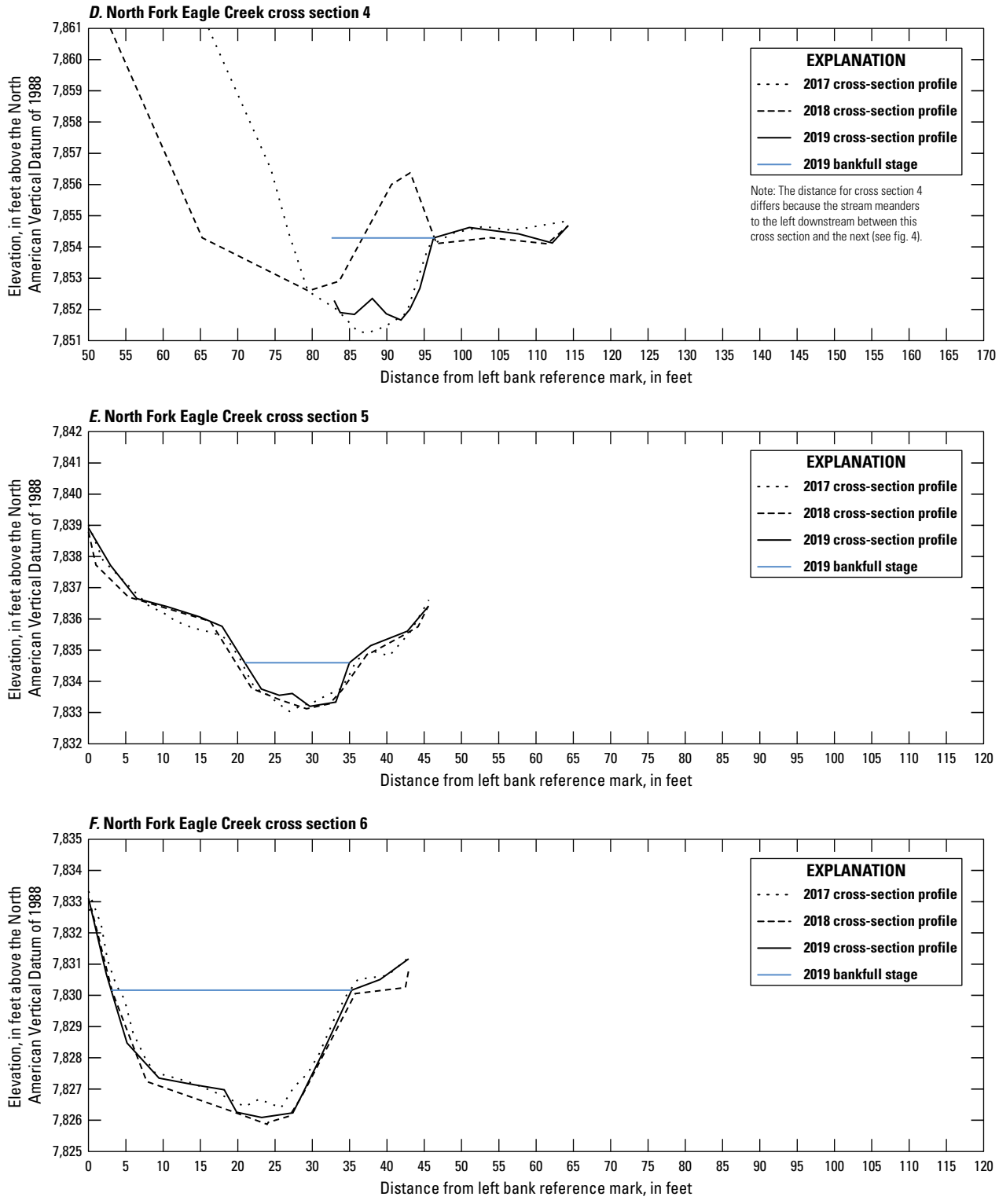


**Figure 7.** Channel cross section 1 to cross section 14 (in downstream order) from the 2017, 2018, and 2019 surveys plotted with 2019 estimates of bankfull stage for the study reach on North Fork Eagle Creek, Eagle Creek Basin, south-central New Mexico. Distances and elevations from 2017 and 2018 have been corrected to the 2019 horizontal and vertical datums on the basis of the differences among the 2017, 2018, and 2019 cross-section reference mark locations and elevations. Areas where there are breaks in the cross-section plots indicate poor quality survey data that were disqualified for use. *A*, Cross section 1. *B*, Cross section 2. *C*, Cross section 3. *D*, Cross section 4. *E*, Cross section 5. *F*, Cross section 6. *G*, Cross section 7. *H*, Cross section 8. *I*, Cross section 9. *J*, Cross section 10. *K*, Cross section 11. *L*, Cross section 12. *M*, Cross section 13. *N*, Cross section 14.—Continued

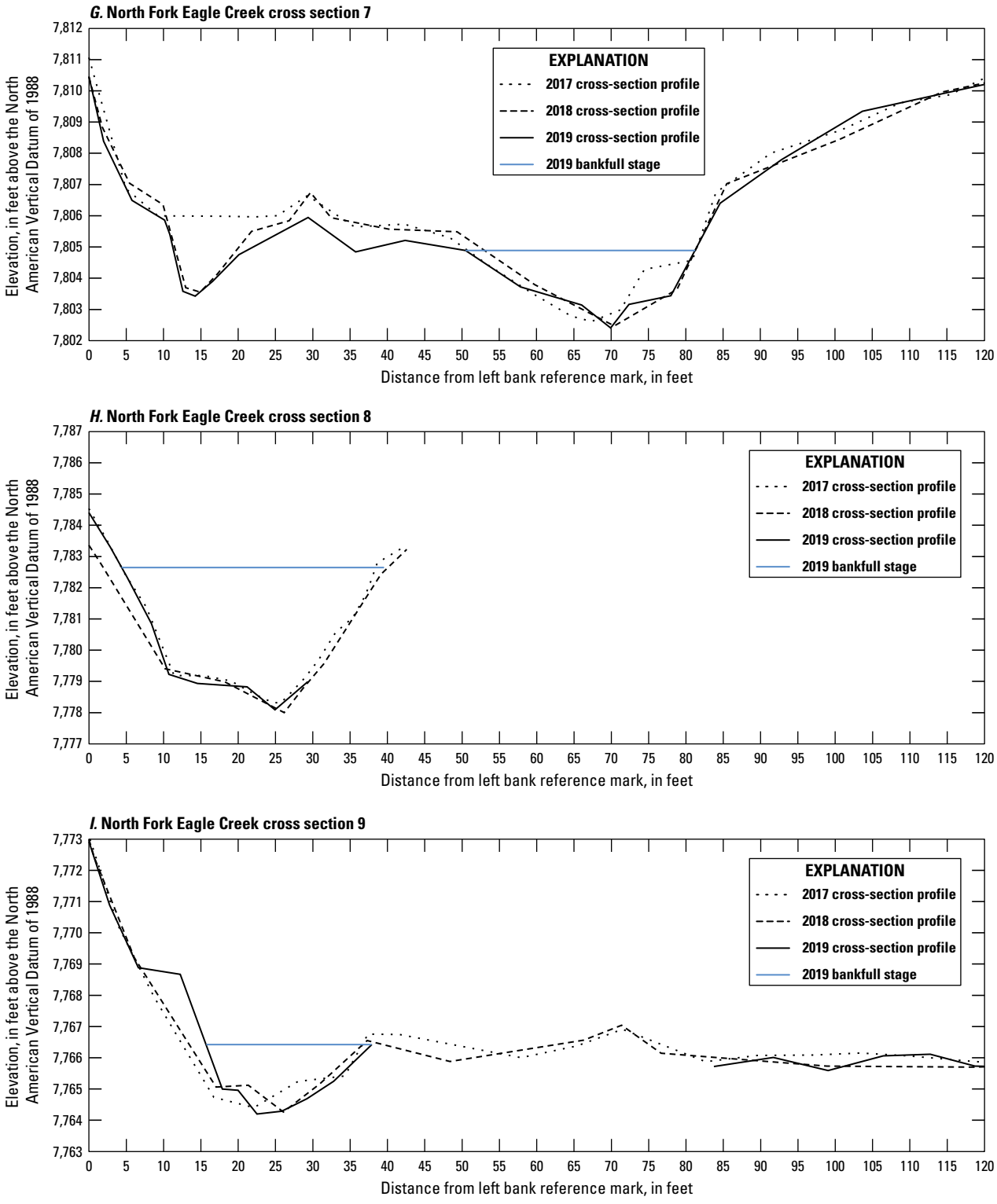


**Figure 7.** Channel cross section 1 to cross section 14 (in downstream order) from the 2017, 2018, and 2019 surveys plotted with 2019 estimates of bankfull stage for the study reach on North Fork Eagle Creek, Eagle Creek Basin, south-central New Mexico. Distances and elevations from 2017 and 2018 have been corrected to the 2019 horizontal and vertical datums on the basis of the differences among the 2017, 2018, and 2019 cross-section reference mark locations and elevations. Areas where there are breaks in the cross-section plots indicate poor quality survey data that were disqualified for use. *A*, Cross section 1. *B*, Cross section 2. *C*, Cross section 3. *D*, Cross section 4. *E*, Cross section 5. *F*, Cross section 6. *G*, Cross section 7. *H*, Cross section 8. *I*, Cross section 9. *J*, Cross section 10. *K*, Cross section 11. *L*, Cross section 12. *M*, Cross section 13. *N*, Cross section 14.—Continued

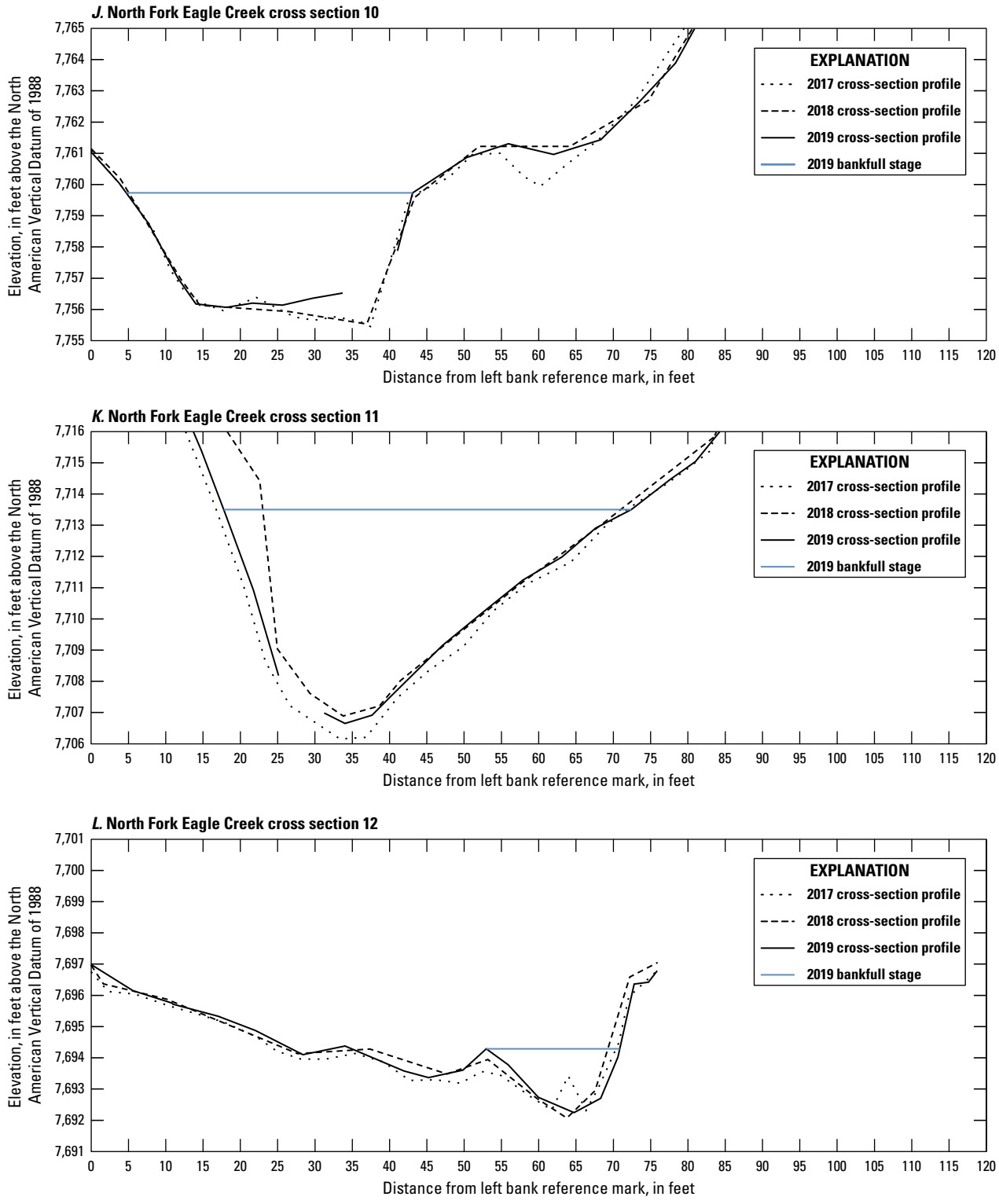


**Figure 7.** Channel cross section 1 to cross section 14 (in downstream order) from the 2017, 2018, and 2019 surveys plotted with 2019 estimates of bankfull stage for the study reach on North Fork Eagle Creek, Eagle Creek Basin, south-central New Mexico. Distances and elevations from 2017 and 2018 have been corrected to the 2019 horizontal and vertical datums on the basis of the differences among the 2017, 2018, and 2019 cross-section reference mark locations and elevations. Areas where there are breaks in the cross-section plots indicate poor quality survey data that were disqualified for use. *A*, Cross section 1. *B*, Cross section 2. *C*, Cross section 3. *D*, Cross section 4. *E*, Cross section 5. *F*, Cross section 6. *G*, Cross section 7. *H*, Cross section 8. *I*, Cross section 9. *J*, Cross section 10. *K*, Cross section 11. *L*, Cross section 12. *M*, Cross section 13. *N*, Cross section 14.—Continued

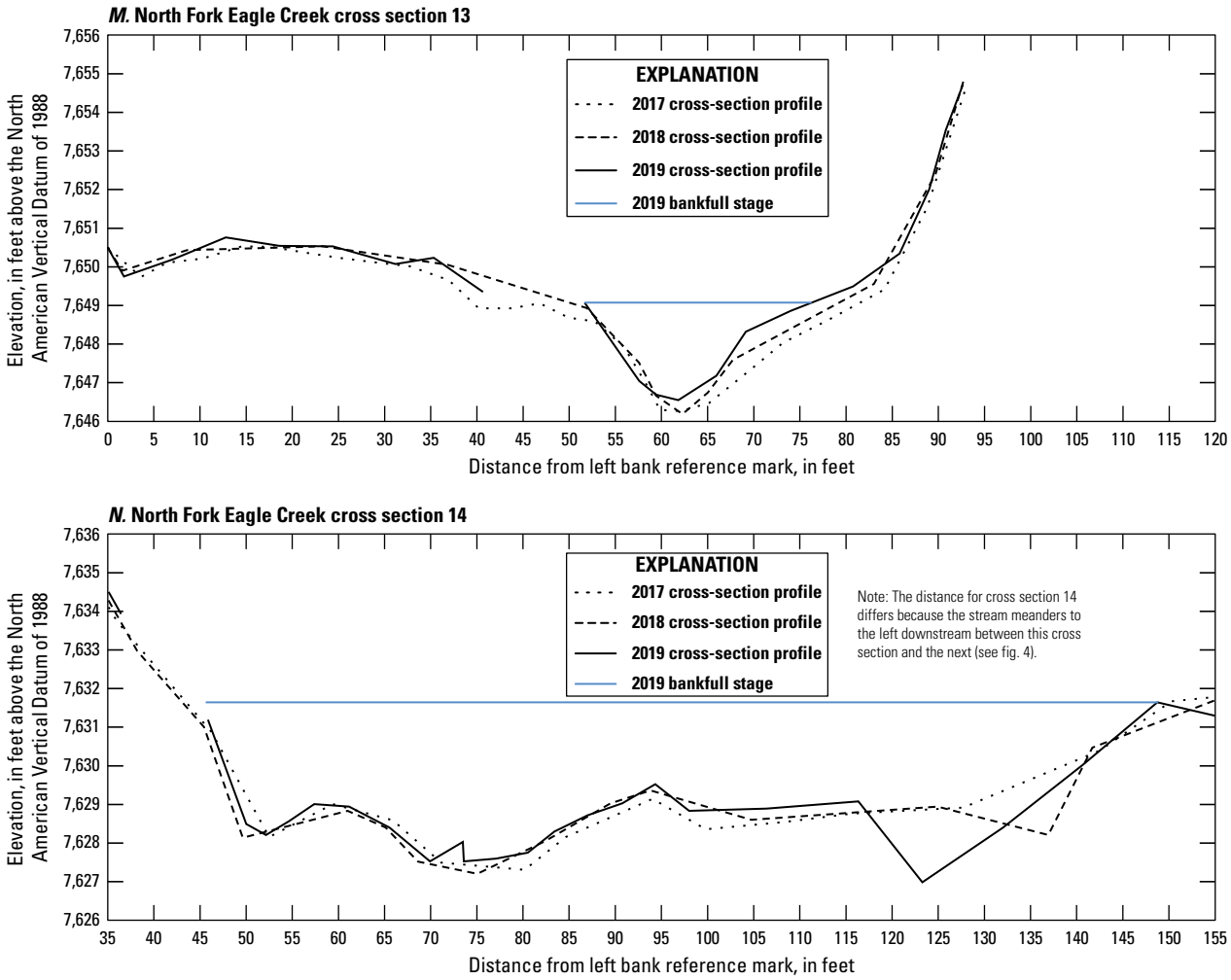


**Figure 7.** Channel cross section 1 to cross section 14 (in downstream order) from the 2017, 2018, and 2019 surveys plotted with 2019 estimates of bankfull stage for the study reach on North Fork Eagle Creek, Eagle Creek Basin, south-central New Mexico. Distances and elevations from 2017 and 2018 have been corrected to the 2019 horizontal and vertical datums on the basis of the differences among the 2017, 2018, and 2019 cross-section reference mark locations and elevations. Areas where there are breaks in the cross-section plots indicate poor quality survey data that were disqualified for use. *A*, Cross section 1. *B*, Cross section 2. *C*, Cross section 3. *D*, Cross section 4. *E*, Cross section 5. *F*, Cross section 6. *G*, Cross section 7. *H*, Cross section 8. *I*, Cross section 9. *J*, Cross section 10. *K*, Cross section 11. *L*, Cross section 12. *M*, Cross section 13. *N*, Cross section 14.—Continued

In the 2018 survey report (Graziano, 2020a), cross sections 2, 4, and 7 were identified as those most likely to have undergone topographic changes (fig. 7*B*, *D*, and *G*). Between 2017 and 2018, it is likely that changes in cross section 2 occurred, but comparable data from the 2019 survey for the right bank were excluded because of high uncertainty in the data collected (fig. 7*B*). Some data from the 2019 survey for cross section 4 were excluded because of uncertainty in the accuracy of survey readings (fig. 7*D*). In cross section 4, it is more likely that the changes are due to problems with the data rather than to channel geomorphology. The survey data for cross section 7 (fig. 7*G*) were complete and indicate that some progressive changes in channel geomorphology are likely occurring.

At cross section 3, between 2017 and 2019 there were changes in the left side of the channel. The left bank of the channel appeared to have eroded by about 1 ft between the 15 and 18 ft horizontal distance marks, and the bed of the channel appeared to have aggraded by about 1 ft between the 20 and 25 ft horizontal distance marks from 2018 to 2019 (fig. 7*C*). Evidence that the left bank of the channel had eroded over the period encompassing the three surveys was shown in photographs taken during the 2017–19 surveys. The photographs showed a left bank defined by a soil surface with little to no vegetation and exposed roots, but more vegetative growth in 2019 on the bank and in the erosional feature suggests that the bank may be stabilizing. Though the plots (fig. 7) show aggradation of the channel bed, changes seen are more likely

**Table 3.** Cross-section characteristics of the study reach on North Fork Eagle Creek, Eagle Creek Basin, south-central New Mexico, 2019.

[ft, foot; ft², square foot; –, not calculated because of poor data quality]

| Cross-section number (fig. 4) | Bankfull stage (ft) | Maximum depth at bankfull stage (ft) | Cross-section channel width (ft) | Cross-section channel area (ft²) | Left bank height (ft) | Left bank slope (dimensionless, ft/ft) | Right bank height (ft) | Right bank slope (dimensionless, ft/ft) |
|---|---|---|---|---|---|---|---|---|
| 1 | 7,898.7 | 2.8 | 35.9 | 50.3 | 2.2 | 0.1 | 2.8 | 0.3 |
| 2 | 7,887.4 | 1.4 | 10.7 | 12.8 | 1.4 | 0.3 | 1.4 | 0.3 |
| 3 | 7,876.2 | 2.5 | 19.4 | 27.7 | 2.2 | 0.8 | 1.8 | 0.3 |
| 4 | 7,854.3 | 2.6 | – | – | – | – | 2.3 | 0.7 |
| 5 | 7,834.6 | 1.4 | 14.0 | 13.6 | 0.8 | 0.4 | 1.3 | 0.7 |
| 6 | 7,830.2 | 4.1 | 32.4 | 90.0 | 2.8 | 0.4 | 3.9 | 0.5 |
| 7 | 7,804.9 | 2.5 | 31.0 | 41.3 | 1.2 | 0.2 | 1.4 | 0.4 |
| 8 | 7,782.6 | 4.6 | – | – | 3.4 | 0.5 | – | – |
| 9 | 7,766.4 | 2.2 | 22.0 | 30.6 | 1.4 | 0.7 | 1.7 | 0.2 |
| 10 | 7,759.7 | 3.7 | 36.9 | – | 3.6 | 0.4 | – | – |
| 11 | 7,713.5 | 6.8 | 54.6 | – | – | – | 6.0 | 0.2 |
| 12 | 7,694.3 | 2.0 | 17.9 | 22.4 | 1.6 | 0.2 | 1.6 | 0.6 |
| 13 | 7,649.1 | 2.5 | 23.8 | 30.9 | 2 | 0.3 | 1.9 | 0.2 |
| 14 | 7,631.6 | 4.7 | – | – | – | – | 3.2 | 0.2 |

due to the accuracy of the survey because the changes fluctuate between degradation between 2017 and 2018 and aggradation between 2018 and 2019. The channel in this cross section contained boulders with diameters greater than 1 ft (some of which appeared to substantially affect the cross-section plot on the right side of the channel). Therefore, the magnitude of the changes in the channel may not actually be as large as the survey results indicated.

At cross section 7, between the 2017 and 2018 surveys, the left side of the channel (between the 5 and 10 ft horizontal distance marks) appeared to have aggraded by about 0.9 ft (fig. 7*G*). The aggradation may be more due to the accuracy of the data rather than to actual change because the 2019 survey data align with the 2017 survey data. Most notably, however, between the 10 and 20 ft horizontal distance marks, part of the right overbank appeared to have degraded by about 2.0 ft. Photographs from the 2018 survey, aerial imagery of the study reach from March 2016, and results from the 2019 survey aligning with results from the 2018 survey in the section of the channel indicate that this degraded section was likely a side channel and not an isolated hole in the ground. Because the aerial imagery was from March 2016, this side channel appeared to already be forming prior to the 2017 survey; however, the survey results indicated that the size of the side channel likely increased between the 2017 and 2019 surveys.

At cross section 10, between the 2017 and 2019 surveys, the right side of the channel (between the 50 and 65 ft horizontal distance marks) appeared to have aggraded by about 1 ft (fig. 7*J*). Photographs taken between the 2017 and 2019 surveys suggest that there was movement of debris in the channel, but more vegetative growth in the channel between the 2018 and 2019 surveys suggests that, if there was water in the channel between surveys, it was likely less energetic and able to deposit sediment.

## Woody Debris

During the 2019 survey, there were 164 distinct accumulations of woody debris identified in the study reach (fig. 8*A*; table 4). Of these, 49 were identified as debris deposits, 19 were identified as potential debris jams, and 96 were identified as active debris jams (fig. 8*A*; table 4). In comparison, in 2019 there were 106 more total accumulations of woody debris than in 2017 and 52 more than in 2018. During the 2018 survey, there were 112 distinct accumulations of woody debris identified in the study reach, with 39 identified as debris deposits, 16 identified as potential debris jams, and 57 identified as active debris jams (Graziano, 2020a). The 2017 survey identified 58 distinct accumulations of woody debris identified in the study reach, with 17 identified as debris deposits, 25 identified as potential debris jams, and 16 identified as active debris jams (Graziano, 2019).

The woody debris accumulation totals from the 2017, 2018, and 2019 surveys varied notably, but there were some similarities found in the spatial distribution of woody debris

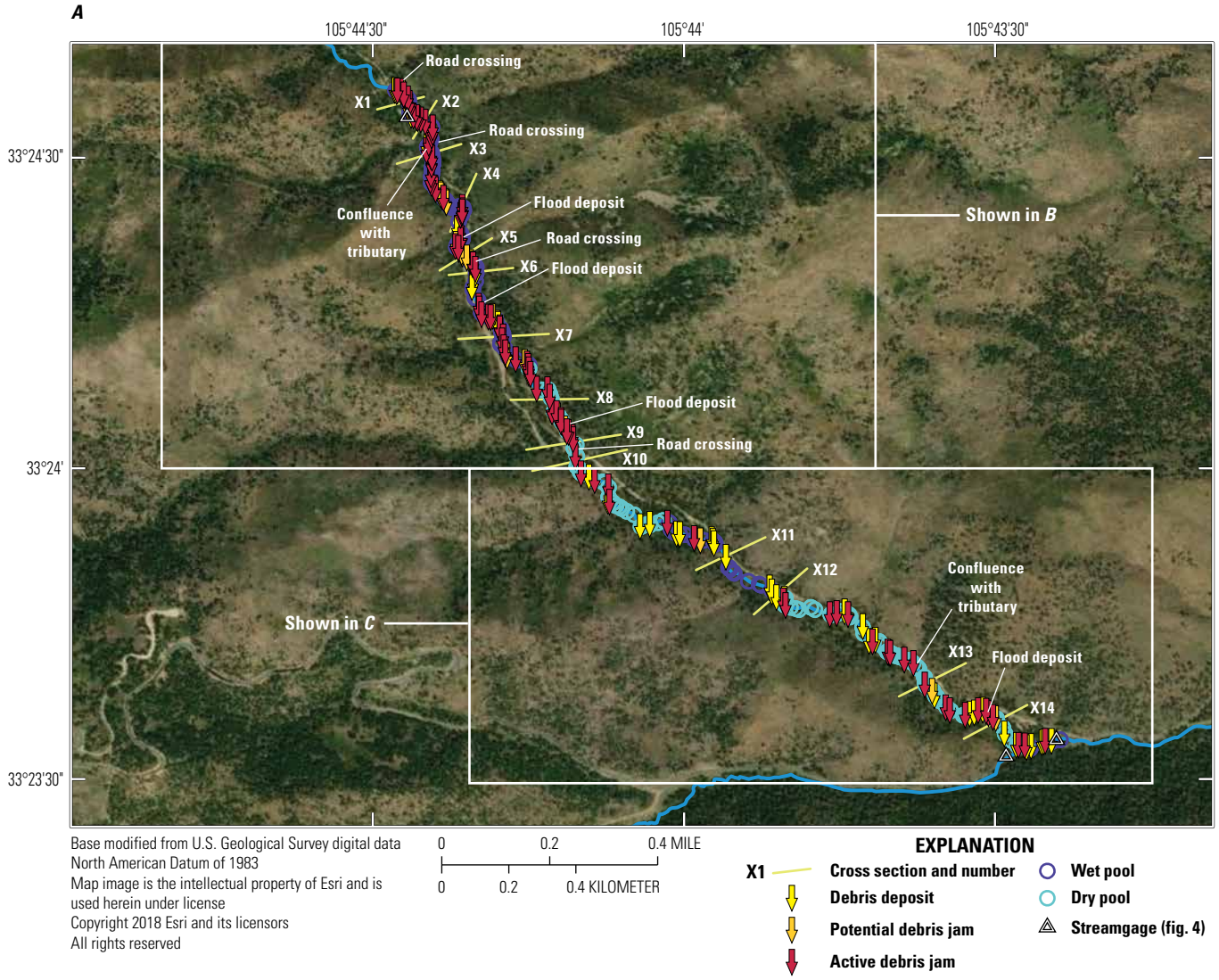


**Figure 8.** Study reach on North Fork Eagle Creek with locations of woody debris accumulations and pools relative to the locations of cross sections, streamgages, and other features in the Eagle Creek Basin, south-central New Mexico, 2019. Cross-section lengths are exaggerated for presentation purposes. *A*, Study reach. *B*, Upstream subreach. *C*, Downstream subreach.

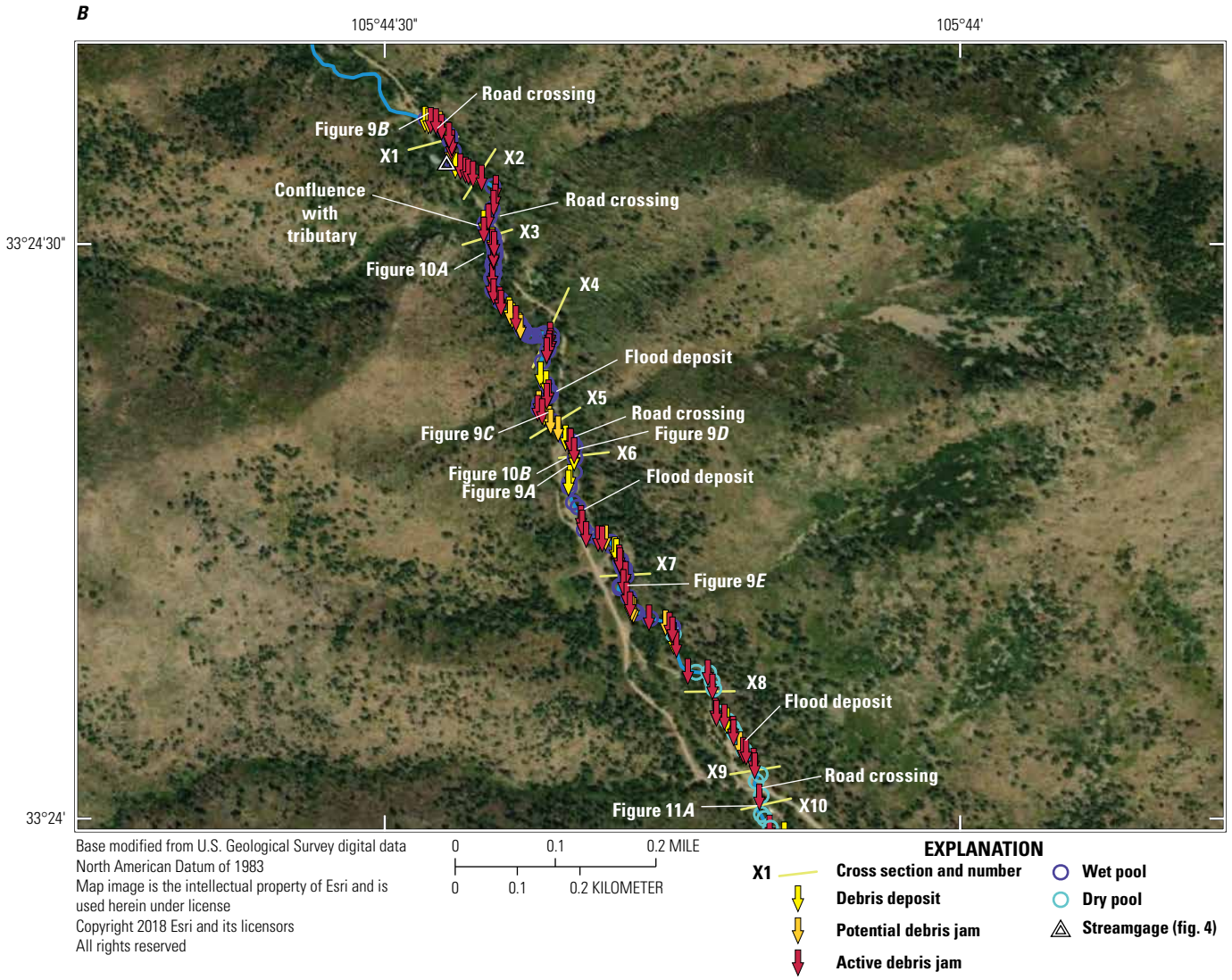


**Figure 8.** Study reach on North Fork Eagle Creek with locations of woody debris accumulations and pools relative to the locations of cross sections, streamgages, and other features in the Eagle Creek Basin, south-central New Mexico, 2019. Cross-section lengths are exaggerated for presentation purposes. *A*, Study reach. *B*, Upstream subreach. *C*, Downstream subreach.—Continued

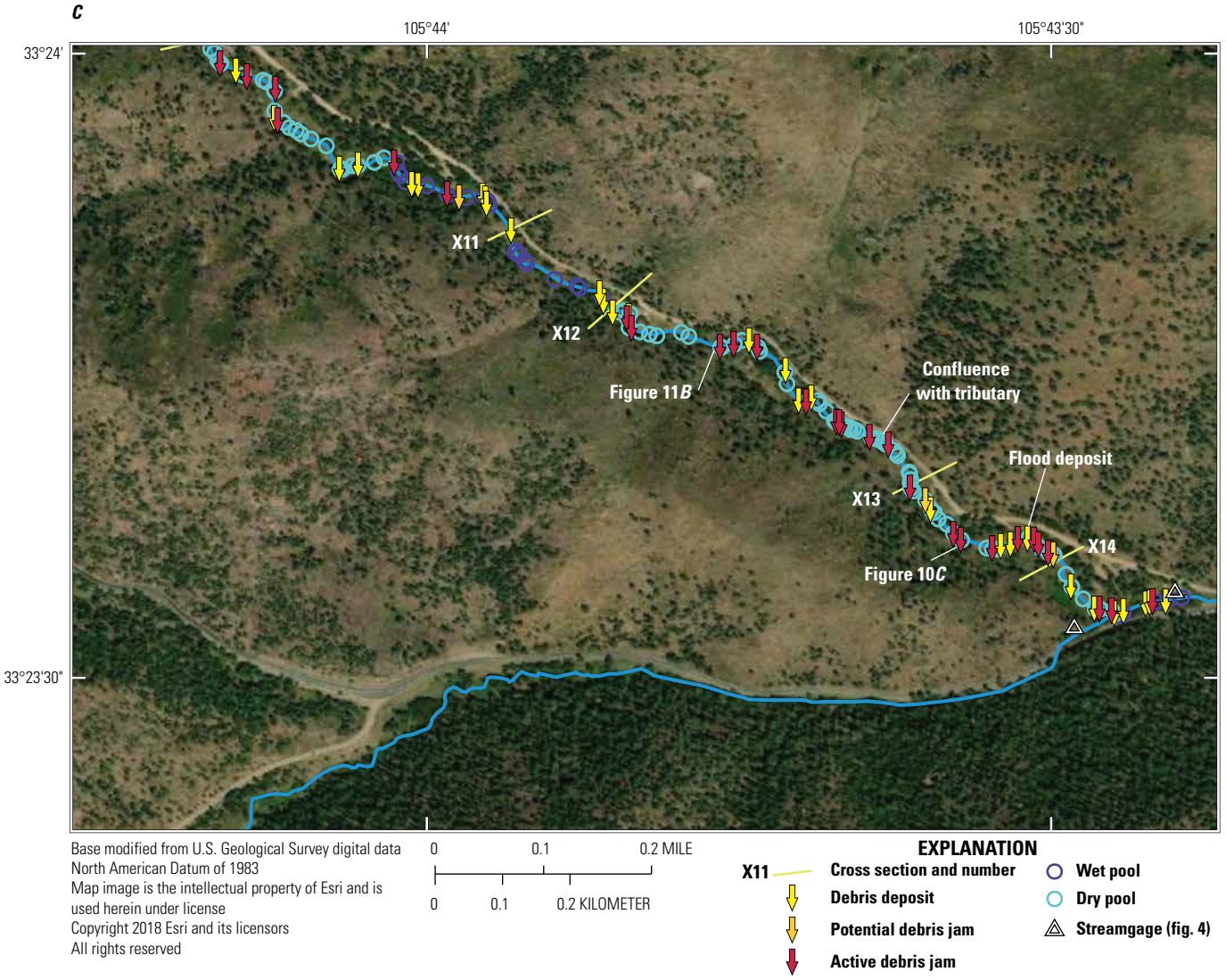


**Figure 8.** Study reach on North Fork Eagle Creek with locations of woody debris accumulations and pools relative to the locations of cross sections, streamgages, and other features in the Eagle Creek Basin, south-central New Mexico, 2019. Cross-section lengths are exaggerated for presentation purposes. *A*, Study reach. *B*, Upstream subreach. *C*, Downstream subreach.—Continued

**Table 4.** Locations, classifications, and average rates of woody debris accumulations identified in the study reach on North Fork Eagle Creek, Eagle Creek Basin, south-central New Mexico, 2019.

[Reach lengths are based on the study reach trace in figure 4 and are rounded to the nearest 5 feet; average rates were calculated for each reach as total number of woody debris accumulations per 1,000 feet; ft, foot; X, cross section]

| Reach | Reach length (ft) | Number of woody debris accumulations by classification | | | Total number of woody debris accumulations | Average rate of woody debris accumulations (per 1,000 ft) |
|---|---|---|---|---|---|---|
| | | Debris deposit | Potential debris jam | Active debris jam | | |
| First road crossing to X1 | 165 | 2 | 2 | 4 | 8 | 48 |
| X1 to X2 | 275 | 1 | 1 | 7 | 9 | 33 |
| X2 to X3 | 385 | 1 | 0 | 6 | 7 | 18 |
| X3 to X4 | 670 | 4 | 2 | 10 | 16 | 24 |
| X4 to X5 | 550 | 3 | 3 | 9 | 15 | 27 |
| X5 to X6 | 200 | 2 | 1 | 3 | 6 | 30 |
| X6 to X7 | 740 | 6 | 1 | 8 | 15 | 20 |
| X7 to X8 | 835 | 2 | 3 | 11 | 16 | 19 |
| X8 to X9 | 465 | 1 | 1 | 9 | 11 | 24 |
| X9 to X10 | 200 | 0 | 0 | 1 | 1 | 5 |
| X10 to X11 | 1,770 | 9 | 1 | 6 | 16 | 9 |
| X11 to X12 | 615 | 2 | 1 | 0 | 3 | 5 |
| X12 to X13 | 1,690 | 5 | 1 | 11 | 17 | 10 |
| X13 to X14 | 790 | 4 | 2 | 8 | 14 | 18 |
| X14 to the Eagle Creek streamgage | 640 | 7 | 0 | 3 | 10 | 16 |
| **Study reach** | **9,990** | **49** | **19** | **96** | **164** | **16** |

accumulations among the three surveys. In 2019, the highest concentration of woody debris accumulations was identified in the upstream subreach, defined here as the reach segment between the first road crossing (located about 165 ft upstream from cross section 1) and cross section 10 (subreach length of about 4,485 ft), where 104 accumulations of woody debris were identified (an average rate of about 25 woody debris accumulations per 1,000 ft) (fig. 8*B*; table 4). In the downstream subreach, defined here as the reach segment between cross section 10 and the Eagle Creek streamgage (subreach length of about 5,505 ft), 60 accumulations of woody debris were identified in 2019 (an average rate of about 11 woody debris accumulations per 1,000 ft) (fig. 8*C*; table 4). In other words, 63 percent of the woody debris accumulations were identified in the upstream subreach, and 37 percent of the woody debris accumulations were identified in the downstream subreach in 2019. In comparison, 60 percent of the woody debris accumulations were identified in the same upstream subreach, and 40 percent were identified in the same downstream subreach in 2018. Similarly, 64 percent of the woody debris accumulations were identified in the same upstream subreach (excluding the 165 ft upstream from cross section 1), and 36 percent were identified in the same downstream subreach in 2017.

Though the distribution of woody debris accumulations between the upstream and downstream subreaches was similar among the 2017 through 2019 surveys, there were some appreciable differences in the distribution of woody debris accumulations within smaller scale cross-section-defined reach segments. Notable differences in number of woody debris accumulations between the 2017 and 2018 surveys were found in the reach segment between cross sections 8 and 11. In that reach segment, only 3 distinct accumulations of woody debris were identified in 2017, and in 2018 there were 27 distinct accumulations of woody debris identified in it (Graziano, 2019, 2020a). There was not much of a change in woody debris accumulations between 2018 and 2019, with the reach segment having 28 distinct accumulations in 2019.

Following the 2019 survey, the most notable differences among the three surveys were found in the reach segment between cross sections 4 and 7. That reach segment has a length of 1,490 ft, and in 2017 there were nine distinct accumulations of woody debris identified in it (Graziano, 2019). In 2018, there were more than twice as many distinct accumulations, with 22 identified in the reach segment (Graziano, 2020a). During the 2019 survey, there were 36 distinct accumulations of woody debris identified in the reach segment (table 4), which is four times as many found in 2017.

As mentioned in Graziano (2020a), methods in counting and classifying woody debris accumulations between the 2017 and 2018 surveys were changed. Through comparison of the locations and photographs of woody debris accumulations from the 2017 and 2018 surveys, it was determined that differences in the woody debris accumulation totals and spatial distributions were primarily due to actual changes that occurred in the study reach and were not due to differences in the application of the methods between the 2017 and 2018 surveys used to identify woody debris accumulations or due to changes in the extent of the study reach (Graziano, 2020a). Specifically, it was determined that there were 49 accumulations of woody debris (11 debris deposits, 7 potential debris jams, and 31 active debris jams) identified in the study reach in 2018 that were not identified in 2017 and likely settled in their 2018 locations sometime between the 2017 and 2018 surveys. Further, there were 34 accumulations of woody debris (16 debris deposits, 15 potential debris jams, and 3 active debris jams) surveyed in 2017 that were not identified in 2018 and were likely transported away from their 2017 locations sometime between the 2017 and 2018 surveys. Graziano (2020a) provided a more in-depth discussion regarding changes due to differences in the application of the methods used to identify woody debris accumulations between the 2017 and 2018 surveys. For the 2019 survey, the same methods used to identify woody debris accumulations in the 2018 survey were applied.

Ultimately, the results indicated that, of the 164 distinct accumulations of woody debris identified in 2019, there were 67 (41 percent) that were certain to have also been present during the 2018 survey and 21 (13 percent) that were certain to have also been present during all three surveys (2017–19). However, some of these woody debris accumulations that remained in place had undergone observable changes to their sizes, compositions, and structures, though they all maintained some woody debris by which they could be recognized, such as their key members.

Of the 67 woody debris accumulations identified during the 2019 survey that were certain to have also been present during the 2018 survey, 53 had the same classification in 2018 (37 active debris jams, 8 potential debris jams, and 8 debris deposits). Of those that changed classification between the 2018 and 2019 surveys, there were two potential debris jams that became active debris jams, seven debris deposits that became an active debris jam, four active debris jams that were downgraded to potential debris jams, and two active debris jams that became debris deposits. These changes in classification were all due to observable changes in the structure and composition of the woody debris accumulations. Regarding the two active debris jams that became debris deposits, large identifiable wood was still present in the accumulations, but the jams appeared to have been broken up, and the larger wood from them was left loosely scattered in about the same location.

Of the 21 woody debris accumulations identified during all three surveys (2017–19), 12 had the same classification in all 3 years (9 active debris jams and 3 potential debris jams). Over the 3 years from 2017 to 2019, the classification of nine deposits changed. Specifically, three deposits that were classified as potential debris jams were changed to active debris jams, three deposits were changed from potential to active debris jams between 2017 and 2018 and then downgraded to potential debris jams in 2019, and three more deposits were either upgraded or downgraded in classification over the years.

Example photographs of different woody debris accumulations identified during the 2019 survey are presented in figure 9, and the locations of the examples are shown in figure 8. Figure 9*A* depicts a type of debris deposit that was commonly seen during the 2019 survey, that being a debris deposit made up of woody debris loosely scattered on the side of the channel rather than in the middle.

Figure 9*B* and *C* shows examples of potential debris jams. In figure 9*B*, a log crosses the channel without causing any jamming in the channel, but the log is low and may become an active debris jam at moderately higher flows. The potential debris jam depicted in figure 9*B* was found upstream from cross section 1, before the first road crossing. Figure 9*C*, found upstream from cross section 5, depicts a less common type of potential debris jam, with potential geomorphic implications. It was one of the seven potential debris jams that was presumed to have newly formed between 2017 and 2018. This potential debris jam was unique in that it was a potential debris jam that appeared to have contributed to visible geomorphic change in the channel; specifically, where the tree uprooted on the left bank, the left bank collapsed, and the channel became constricted. It was also unique because it can be said with certainty that it was not woody debris that was mobilized and deposited by streamflow. Further, because the tree was large (between 2 and 3 ft in diameter) and it appeared to be firmly anchored by its root structure, it is likely that it will remain in place unless there is a substantial increase in streamflow or it is removed by artificial means. Therefore, it is likely well suited to become the key member of an active debris jam and to continue to be a driver of geomorphic change in the location where it was found during the 2018 survey.

Figure 9*D* and *E* depicts active debris jams with characteristics that were common to most of the active debris jams identified in the study reach in 2019. Specifically, the active debris jam in figure 9*D*, found upstream from cross section 6, contained small woody debris packed tightly against LWD key members, mostly on the upstream side. Also, like in most other active debris jams identified in 2019, the key members do not appear to be firmly anchored; therefore, the active debris jam could be easily mobilized and transported by high flows. Figure 9*E* (downstream from cross section 7) depicts an active debris jam that appeared to be the largest (by volume) found in the study reach in 2019 and that was also identified in 2018. This active debris jam is located downstream from cross section 7 and does not appear to have changed from 2018 to 2019, possibly because flows were not substantial enough to move debris.


**Figure 9.** Examples of woody debris accumulations identified in the study reach on North Fork Eagle Creek, Eagle Creek Basin, south-central New Mexico, 2019. All photographs are oriented downstream. For scale, a survey rod that is 4.46 feet in length (with graduation at feet, tenths of feet, and hundredths of feet) was included in each photograph. Locations of examples are shown in figure 8. *A*, Debris deposit. *B*, Potential debris jam. *C*, Potential debris jam. *D*, Active debris jam. *E*, Active debris jam.

**Table 5.** Locations, residual depth classifications, dry or wet indications, and average rates of pools identified in the study reach on North Fork Eagle Creek, Eagle Creek Basin, south-central New Mexico, 2019.

[Reach lengths are based on the study reach trace in figure 4 and are rounded to the nearest 5 feet; average rates were calculated for each reach as total number of pools per 1,000 feet; ft, foot; <, less than; >, greater than; X, cross section]

| Reach | Reach length (ft) | Number of pools by residual depth classification | | | Total number of dry pools | Total number of wet pools | Total number of pools | Average rate of pools (per 1,000 ft) |
|---|---|---|---|---|---|---|---|---|
| | | Shallow (<0.75 ft) | Intermediate (0.75–1.25 ft) | Deep (>1.25 ft) | | | | |
| First road crossing to X1 | 165 | 12 | 0 | 0 | 0 | 12 | 12 | 73 |
| X1 to X2 | 275 | 6 | 1 | 1 | 0 | 8 | 8 | 29 |
| X2 to X3 | 385 | 5 | 1 | 0 | 0 | 6 | 6 | 16 |
| X3 to X4 | 670 | 30 | 2 | 0 | 0 | 32 | 32 | 48 |
| X4 to X5 | 550 | 14 | 0 | 0 | 0 | 14 | 14 | 25 |
| X5 to X6 | 200 | 4 | 1 | 0 | 0 | 5 | 5 | 25 |
| X6 to X7 | 740 | 16 | 0 | 0 | 0 | 16 | 16 | 22 |
| X7 to X8 | 835 | 10 | 2 | 2 | 5 | 9 | 14 | 17 |
| X8 to X9 | 465 | 2 | 2 | 1 | 5 | 0 | 5 | 11 |
| X9 to X10 | 200 | 1 | 1 | 1 | 3 | 0 | 3 | 15 |
| X10 to X11 | 1,770 | 8 | 18 | 6 | 21 | 11 | 32 | 18 |
| X11 to X12 | 615 | 6 | 3 | 0 | 0 | 9 | 9 | 15 |
| X12 to X13 | 1,690 | 12 | 19 | 12 | 43 | 0 | 43 | 25 |
| X13 to X14 | 790 | 0 | 11 | 5 | 16 | 0 | 16 | 20 |
| X14 to the Eagle Creek streamgage | 640 | 7 | 3 | 3 | 7 | 6 | 13 | 20 |
| **Study reach** | **9,990** | **133** | **64** | **31** | **100** | **128** | **228** | **23** |

## Pools

During the 2019 survey, there were 228 pools identified in the study reach (fig. 8; table 5). Of the 228 pools identified, 151 were identified in the dry section of the study reach (which is the lower 1.45 mi of the study reach that begins about 100 ft downstream from cross section 6), and 77 were identified in the wet section of the study reach (which is the upper 0.44 mi of the study reach) (fig. 8*A*; table 5). Residual depths for all pools ranged from 0.15 ft (one pool in the reach segment between the first road crossing and cross section 1) to 3 ft (one pool in the reach segment about 50 ft upstream from cross section 10, in the dry section of the study reach) (Graziano and Chavarria, 2022). On the basis of their residual depths, 133 pools were classified as shallow (less than 0.75 ft), 64 were classified as intermediate (0.75–1.25 ft), and 31 were classified as deep (greater than 1.25 ft) (table 5).

As mentioned in Graziano (2020a), the methods for identifying pools in the 2017 survey were adjusted, and identification of pools in the 2019 survey followed the methods used in the 2018 survey. Thus, a direct comparison between pools surveyed in 2018 and 2019 can be made, but only general comparisons between the 2017 survey pool data and subsequent survey pool data can be made.

In the 2019 survey, 115 pools were identified in the 0.85 mi upstream subreach (an average rate of about 28 pools per 1,000 ft) (fig. 8*B*; table 5), and 113 pools were identified in the 1.04 mi downstream subreach (an average rate of about 20 pools per 1,000 ft) (fig. 8*C*; table 5). In comparison, in the 2018 survey, 39 pools were identified in the 0.85 mi upstream subreach (an average rate of about 9 pools per 1,000 ft), and 32 pools were identified in the 1.04 mi downstream subreach (an average rate of about 6 pools per 1,000 ft) (Graziano, 2020a). In both 2018 and 2019, the maximum number of pools in the upstream subreach was found in the reach segment between cross sections 3 and 4. In this reach segment, 32 pools were found in 2019, and 12 pools were found in 2018; nearly all pools were classified as shallow (less than 0.75 ft residual depth) in both years. The maximum number of pools (14 pools) in the downstream subreach in 2018 was found in the reach segment between cross sections 10 and 11, whereas in 2019 the maximum number of pools (43 pools) was found in the reach segment between cross sections 12 and 13. In 2018, nearly half of the pools found in the reach segment between cross sections 12 and 13 were classified as shallow, and the other half were classified as deep (greater than 1.25 ft


**Figure 10.** Examples of pools identified in the study reach on North Fork Eagle Creek, Eagle Creek Basin, south-central New Mexico, 2019. All photographs are oriented downstream. Locations of examples are shown in figure 8. *A*, Series of wet pools, which were found between 30 and 100 feet downstream from cross section 3 and photographed with parts of nearby woody debris accumulations. *B*, Wet pool, which was identified in 2019 for the first time and was classified as a shallow pool found at cross section 6. *C*, Dry pool, which was classified as deep (residual depth of greater than 1.25 feet) and also identified during both the 2017 and 2018 surveys found 350 feet downstream from cross section 13.

residual depth); in 2019, a majority of the pools found in the reach segment between cross sections 12 and 13 were classified as intermediate (0.75–1.25 ft residual depth).

During the 2017 survey, only 14 pools were identified in the study reach; they were not measured for residual depth, and they were identified in only the upper two-thirds of the study reach (Graziano, 2019). Because methods for identifying and measuring pools had not been well established prior to the 2017 survey, it is likely that many of the shallower pools in the study reach, especially in the dry sections, were overlooked in 2017; therefore, the pool totals from 2017 and from 2018 through 2019 are not presumed to be directly comparable. However, there were some general similarities in the distributions of pools seen during the 2017 survey that were seen during the 2018 and 2019 surveys. Specifically, in 2017, like in 2018 and 2019, relatively dense clusters of pools were identified between cross sections 3 and 4 in the upstream subreach. In the downstream subreach, the maximum number of pools found in 2017 was in the reach segment between cross sections 11 and 12, in the same section in which the maximum number of pools was found in 2019.

Between the 2018 and 2019 surveys, there were changes to the pools in the study reach. The changes were determined through comparison of the locations and photographs of pools from the 2018 and 2019 surveys. For example, there were 54 pools that were identified in both 2018 and 2019 and at least 17 pools that were identified in 2018 but not in 2019. Pools identified during the 2018 survey that were not identified during the more thorough 2019 survey likely filled in or physically changed in some other way that prevented them from being identified as pools in 2019.

Example photographs presented in figure 10 depict various characteristics of pools identified in the study reach during the 2019 survey (locations of the examples are shown in fig. 8). Figure 10*A* depicts two pools classified as intermediate with respect to residual depth (table 5) that were located about 50 ft downstream from cross section 3; these pools were also present during the 2018 survey. Figure 10*B* (at cross section 6) shows a new pool that was found in 2019 and classified as a shallow pool. Figure 10*C* depicts a dry pool that was colocated with an active debris jam that may have influenced its

formation. The pool depicted in figure 10*C* was found about 350 ft downstream from cross section 13 and classified as a deep pool.

## Other Features of Geomorphic Significance

During both the 2018 and 2019 surveys, four road crossings, four flood deposits, and two tributary confluences were identified (figs. 4 and 8). Unless major flooding occurs, both the locations and numbers of road crossings and flood deposits are expected to remain the same through the five planned surveys. Additionally, the two identified tributary confluences are expected to remain in the same locations through the five planned surveys. However, more tributary confluences may be identified during future surveys because tributary confluence identification was not rigorous and was entirely based either on the presence of water in the tributary or on the presence of engineered structures, such as culverts. During periods when streamflow is higher than it was during the 2017–19 surveys, there are likely other tributaries contributing streamflow to the study reach. Though the identified road crossings, flood deposits, and tributary confluences are all expected to remain in the same locations through the five planned surveys, their locations may become important to understanding the geomorphic processes active during the surveys.

During the 2019 survey, 13 channel bifurcations and 30 fine-sediment accumulations were identified. The survey of bifurcations and fine-sediment accumulations was more in depth in 2019 than it was in 2018, and of the 13 bifurcations found in 2019, 4 of those were also identified in 2018. Of the 30 fine-sediment accumulations found in 2019, 7 of them were also present in 2018. An examination of field photographs suggests that at least nine of the bifurcations found in 2019 were present in 2018, but because these features were not rigorously identified, it is likely that not all of the channel bifurcations or fine-sediment accumulations in the study reach were cataloged. In addition, channel bifurcations in dry sections of the channel, especially those in the larger flood deposits, could be difficult to identify, primarily because there was not always a clear path that streamflow would follow, and in the larger flood deposits, some sections of the channel appeared to be braided and separated into more than two distributaries instead of bifurcated into only two distinct channels. The identification of fine-sediment accumulations was also affected by the local stream characteristics but in different ways. Specifically, fine-sediment accumulations were only observed in dry sections of the study reach and may have been overlooked both in flood deposits and in areas where water was present.

Example photographs presented in figure 11 depict characteristics of channel bifurcations and fine-sediment accumulations identified in the study reach during the 2019 survey (locations of the examples are shown in fig. 8). Figure 11*A* depicts a channel bifurcation that was about 50 ft long (channelwise) and had no woody debris present. This bifurcation was also identified in 2018 and had a debris deposit in it. Figure 11*B* depicts a fine-sediment accumulation that was colocated with a woody debris pile, which may have slowed water enough for sediment to settle.


**Figure 11.** Examples of channel bifurcations and fine-sediment accumulations identified in the study reach on North Fork Eagle Creek, Eagle Creek Basin, south-central New Mexico, 2019. All photographs are oriented downstream. For scale, a survey rod that is 4.46 feet in length (with graduation at feet, tenths of feet, and hundredths of feet) was included in one of the photographs. Locations of examples are shown in figure 8. *A*, Channel bifurcation, which was about 50 feet long. *B*, Fine-sediment accumulation, colocated with a debris pile.

# The Geomorphic Implications of the Hydrologic Responses to the 2012 Little Bear Fire and the Potential for Future Geomorphic Change to North Fork Eagle Creek

The 2012 Little Bear Fire caused substantial loss of vegetation in the North Fork Eagle Creek Basin. The loss of vegetation and other potential fire effects were expected to cause hydrologic responses that included reduced infiltration and increased overland runoff, temporary increases in "flashy" responses to rainfall and snowmelt, increased sediment and debris yields, and changes to vegetation from flooding (USDA Forest Service, 2016). The results from the first three of five planned geomorphic surveys of North Fork Eagle Creek, presented in this report and in Graziano (2019, 2020a), have been used to assess some of these expected hydrologic responses, to monitor geomorphic change to North Fork Eagle Creek, and to provide baseline data for future geomorphic monitoring of North Fork Eagle Creek. In this section, these expected hydrologic responses and their geomorphic implications are discussed (with the exception of changes to vegetation from flooding). Further, on the basis of data collected thus far, the hypotheses made in Graziano (2019) about the potential for future geomorphic change to North Fork Eagle Creek are assessed.

In Graziano (2019), the expected hydrologic responses of reduced infiltration, increased overland runoff, and "flashy" responses to rainfall and snowmelt were assessed by using the peak annual streamflow records from the North Fork and Eagle Creek streamgages. Though only 5 years of data were collected since the Little Bear Fire (and at the North Fork streamgage, only 5 years of data were collected before the Little Bear Fire), the peak annual streamflow records examined in Graziano (2019) indicate a flashy response to rainfall and snowmelt in some instances. Though, it is important to note that without long-term streamflow and precipitation data it is difficult to determine if the flashy or high-flow events are within the historical range of variability. Graziano (2019) found that peak annual streamflows of relatively high magnitude (greater than 50.00 $ft^3/s$) had most commonly occurred during the North American monsoon season (both before and after the Little Bear Fire), indicating that most peak annual streamflows had been caused by rainfall rather than snowmelt. Therefore, it was hypothesized in Graziano (2019) that, if observable geomorphic change occurs in the study reach during the 5 years planned for the study, there is a strong possibility that it will have been caused by rainfall during the months of the North American monsoon season (July, August, and September). The streamflow records analyzed in this report, from the period between the 2017 and 2018 surveys, partially supported this hypothesis because the "flashiest" high-flow event at the Eagle Creek streamgage (with a peak instantaneous streamflow greater than 50.00 $ft^3/s$) occurred during the North American monsoon season, and that high-flow event likely made some contributions to the geomorphic changes that occurred in the study reach between the 2017 and 2018 surveys. However, the highest magnitude peak instantaneous streamflow with the longest period of sustained high flows in the study reach (for the period starting on the last day of the 2018 survey and ending on the last day of the 2019 survey [June 14, 2018–June 20, 2019]) occurred in the month of January (fig. 5*A* and *B*). It is likely that either a rapid increase in temperature or a rain-on-snow event could have caused the peak in streamflow, but a closer examination of precipitation and temperature data would be needed to confirm that the peak was a result of rapid snow melt. In addition, streamflows of lower magnitude (less than 50.00 $ft^3/s$) occurred from February through March and had presumably been caused by snowmelt runoff, but the magnitude of streamflows likely only contributed to minor geomorphic changes observed in the reach during the 2019 survey.

Graziano (2019) suggested that long periods during which streamflow remained less than 2.00 $ft^3/s$ in the study reach, prior to the 2017 survey, indicated that it was possible that neither rainfall nor snowmelt would be substantial enough to cause observable geomorphic change in the study reach over the course of the five planned surveys. However, streamflows much greater than 2.00 $ft^3/s$ did occur in the study reach after the 2017 survey, and they did appear to have caused some observable geomorphic change in the study reach.

Limited annual monitoring of increases in sediment and debris yields (which were also expected hydrologic responses to the 2012 Little Bear Fire) began with the 2017 geomorphic survey of North Fork Eagle Creek and continued with the 2018 and 2019 geomorphic surveys of North Fork Eagle Creek. From 2017 to 2019, sediment yields were monitored through repeat surveys of select cross sections of the study reach of North Fork Eagle Creek. Physical changes were identified in only 3 of the 14 cross sections that were surveyed in 2017 and 2018 and in only 4 of the 14 cross sections that were surveyed in 2019, with the most substantial changes appearing to have been caused by channel degradation. However, in 2019 there appeared to be more vegetation in the stream channel and along the banks than in previous years, which would be expected to reduce the amount of sediment loss to erosion. Because there have been many limitations to the postwildfire sediment yield monitoring efforts, it cannot be concluded that sediment yields did not increase or continue to be higher than normal as a result of the fire. Sediment yield monitoring efforts have included the limitations that sediment accumulation outside of the 14 cross-section locations has not been monitored (and was only minimally surveyed in 2018), that sediment transport has not been monitored, and that monitoring of sediment accumulation only began 5 years after the fire.

From 2017 to 2019, debris yields were limitedly monitored through the surveying of woody debris accumulations in the channel of the study reach. Between the 2017 and 2018 surveys, it was found that high flows that occurred between

the surveys were able to mobilize woody debris in the channel, and though some woody debris accumulations identified in 2018 may have been overlooked in 2017, the total number of woody debris accumulations in the channel appeared to increase between the two surveys. Between the 2018 and 2019 surveys there were more instances of moderate flows (greater than 2.00 $ft^3/s$ but less than 50.00 $ft^3/s$) at the North Fork and Eagle Creek streamgages and more woody debris accumulations found as a result. The greatest difference in woody debris among all three surveys was found in the reach segment between cross sections 4 and 7. There were nearly four times as many accumulations found in 2019 than in 2017. In addition, in both 2018 and 2019, cross section 7 was also found to have likely undergone geomorphic change due to fluvial processes. Therefore, it is likely that woody debris influenced the geomorphic change seen in cross section 7 but likely had minimal effects at other locations.

During the 2019 geomorphic survey, 228 pools were found in the study reach by using methods significantly refined from those used during the 2017 survey. Because the methods were refined, direct comparisons among the 2017 survey and subsequent surveys were not possible.

During the 2017 geomorphic survey, 14 pools were found in the study reach (Graziano, 2019), and during the 2018 geomorphic survey, 71 pools were found in the study reach (Graziano, 2020a). Comparisons between the 2018 and 2019 surveys of pools indicate that there were more pools found in total but that the relative size of pools remained mostly the same. For example, in both 2018 and 2019, shallow pools were the greatest number of pools found, and deep pools were the least number of pools found. In Graziano (2019), it was hypothesized that the identified pools would likely remain in place, with the same general size and structure, unless flow events of a particularly high magnitude occurred. As mentioned above in this section, there were more instances of moderate flows (greater than 2.00 $ft^3/s$ but less than 50.00 $ft^3/s$) in the sections of the study reach. There were 54 pools that were found in 2019 that were also found in 2018 and at least 17 pools that were found in 2018 that were not found in 2019, thereby indicating that the moderate flows may have influenced the number of pools found. Plans for future surveys of the study reach include continued use of those pool identification and measurement methods that were refined for the 2018 survey; therefore, it is expected to be much less likely for new pools to be identified during future surveys (in wet or dry sections of the study reach) unless they newly form during the remaining years of the planned surveys.

# Summary

About one-quarter of the water supply for the Village of Ruidoso, New Mexico, is from groundwater pumped from wells located along North Fork Eagle Creek in the National Forest System lands of the Lincoln National Forest near Alto, N. Mex. Because of concerns regarding the effects of groundwater pumping on surface-water hydrology in the North Fork Eagle Creek Basin and the effects of the 2012 Little Bear Fire, which resulted in substantial loss of vegetation in the basin, the U.S. Department of Agriculture Forest Service, Lincoln National Forest, has required monitoring of a portion of North Fork Eagle Creek for geomorphic change as part of the permitting decision that allows for the continued pumping of the production wells. The objective of this study is to address the geomorphic monitoring requirements of the permitting decision by conducting annual geomorphic surveys of North Fork Eagle Creek along the stream reach between the North Fork Eagle Creek near Alto, N. Mex., streamgage (U.S. Geological Survey [USGS] site 08387550) and the Eagle Creek below South Fork near Alto, N. Mex., streamgage (USGS site 08387600). The monitoring of geomorphic change in the stream reach began in June 2017 with surveys of select cross sections and surveys of all woody debris accumulations and pools identified in the channel. In June 2018 and 2019, the monitoring of geomorphic change continued with two more geomorphic surveys of the stream reach (with some modification to the monitoring methods).

The 2017, 2018, and 2019 surveys were conducted by the USGS, in cooperation with the Village of Ruidoso, and were the first three in a planned series of five annual geomorphic surveys. The results of the 2017 and 2018 geomorphic surveys were summarized and interpreted in previous USGS open-file reports, and the data were published in the companion data releases of those reports. In this report, the results of the 2019 geomorphic survey are summarized, interpreted, and compared to the results of the 2017 and 2018 surveys. The data from the 2019 geomorphic survey are published in the companion data release of this report.

The study reach surveyed in June 2019 is 1.89 miles long, beginning about 260 feet upstream from the North Fork Eagle Creek near Alto, N. Mex., streamgage and ending at the Eagle Creek below South Fork near Alto, N. Mex., streamgage. Large sections of the study reach are characterized by intermittent streamflow, and where streamflow is normally continuous (including at the upper and lower portions of the study reach, near the streamgages), the streamflow typically remains less than 2.00 cubic feet per second throughout the year except during seasonal high flows, which most often result from rainfall during the North American monsoon season months of July, August, and September or from snowmelt runoff in March, April, and May. During 2017–19, high-flow events resulting from both rainfall (during the North American monsoon season) and snowmelt runoff (during the winter) occurred in the study reach, and those high-flow events appeared to have caused some minor and localized geomorphic changes in the study reach, which were evaluated through comparison of the 2017, 2018, and 2019 survey results.

For the 2017 geomorphic survey of North Fork Eagle Creek, cross sections were established and surveyed at 14 locations along the study reach, and in 2018 and 2019, those same 14 cross sections were resurveyed. Comparisons of the

cross-section survey results suggest that minor observable geomorphic changes had occurred in 4 of the 14 cross sections. These minor observable geomorphic changes included aggradation or degradation of surface materials by about 1–2 feet in some parts of the affected cross sections.

To further assess geomorphic changes within the study reach, other features, including woody debris accumulations and pools, were surveyed in 2017, 2018, and 2019. During the 2019 geomorphic survey, 164 distinct accumulations of woody debris and 228 pools were identified in the study reach. Of the woody debris accumulations identified during the 2019 survey, 67 were certain to have also been present during the 2018 survey, and 21 were certain to have also been present during all three surveys (2017–19), indicating that most of the woody debris accumulations surveyed in 2017 were likely transported during the high-flow events between the 2017 and 2018 surveys but also indicating that the streamflow during those events was not high enough to remove some of the more firmly anchored woody debris accumulations. Most woody debris accumulations identified in 2019 did not appear to have substantially influenced geomorphic change in the locations where they were found. However, the identification of more woody debris accumulations and pools in the study reach in 2019 may have been the result of more instances of moderate streamflows occurring during the winter season, which may have driven local geomorphic changes. Notably, pool totals from the 2017 survey could not be accurately compared to the pool totals from the 2018 and 2019 surveys because of differences between the 2017 survey and the 2018 and 2019 surveys in the methods used to identify pools.

Because the study began 5 years after the 2012 Little Bear Fire and the geomorphic scope of the study has so far been limited, it cannot be said that the geomorphic changes observed among the three surveys (2017–19) are representative of a pattern of geomorphic change to North Fork Eagle Creek following the 2012 Little Bear Fire. Though, once geomorphic changes identified during the five planned surveys can be compared, it may be possible to develop an understanding of the patterns in geomorphic change to North Fork Eagle Creek following the fire.

## Acknowledgments

Matthew Pedroza, U.S. Geological Survey, assisted with the field work.

## References Cited

Abbe, T.B., and Montgomery, D.R., 1996, Large woody debris jams, channel hydraulics and habitat formation in large rivers: Regulated Rivers, v. 12, no. 2–3, p. 201–221, accessed April 19, 2018, at https://doi.org/10.1002/(SICI)1099-1646(199603)12:2/3<201::AID-RRR390>3.0.CO;2-A.

Benson, M.A., and Dalrymple, T., 1967, General field and office procedures for indirect measurements: U.S. Geological Survey Techniques of Water-Resources Investigations, book 3, chap. Al, 30 p., accessed August 8, 2018, at https://doi.org/10.3133/twri03A1.

Bradley, D.N., 2012, Slope-area computation program graphical user interface 1.0—A preprocessing and postprocessing tool for estimating peak flood discharge using the slope-area method: U.S. Geological Survey Fact Sheet 2012–3112, 4 p., accessed July 26, 2018, at https://pubs.usgs.gov/fs/2012/3112.

Buffington, J.M., Lisle, T.E., Woodsmith, R.D., and Hilton, S., 2002, Controls on the size and occurrence of pools in coarse-grained forest rivers: River Research and Applications, v. 18, no. 6, p. 507–531, accessed May 4, 2018, at https://doi.org/10.1002/rra.693.

Dalrymple, T., and Benson, M.A., 1968, Measurement of peak discharge by the slope-area method: U.S. Geological Survey Techniques of Water-Resources Investigations, book 3, chap. A2, 12 p., accessed August 8, 2018, at https://doi.org/10.3133/twri03A2.

Fulford, J.M., 1994, User's guide to SAC, a computer program for computing discharge by slope-area method: U.S. Geological Survey Open-File Report 94–360, 31 p., accessed July 26, 2018, at https://doi.org/10.3133/ofr94360.

Graziano, A.P., 2018, Data supporting the 2017 geomorphic survey of North Fork Eagle Creek, New Mexico: U.S. Geological Survey data release, accessed August 29, 2019, at https://doi.org/10.5066/F7PR7TX3.

Graziano, A.P., 2019, Geomorphic survey of North Fork Eagle Creek, New Mexico, 2017: U.S. Geological Survey Open-File Report 2018–1187, 28 p., accessed March 15, 2022, at https://doi.org/10.3133/ofr20181187.

Graziano, A.P., 2020a, Geomorphic survey of North Fork Eagle Creek, New Mexico, 2018: U.S. Geological Survey Open-File Report 2020–1121, 37 p., accessed March 15, 2022, at https://doi.org/10.3133/ofr20201121.

Graziano, A.P., 2020b, Data supporting the 2018 geomorphic survey of North Fork Eagle Creek, New Mexico: U.S. Geological Survey data release, accessed March 15, 2022, at https://doi.org/10.5066/P94ZQHKU.

Graziano, A.P., and Chavarria, S.B., 2022, Data supporting the 2019 geomorphic survey of North Fork Eagle Creek, New Mexico: U.S. Geological Survey data release, https://doi.org/10.5066/P97ALYNZ.

Gurnell, A.M., Piegay, H., Swanson, F.J., and Gregory, S.V., 2002, Large wood and fluvial processes: Freshwater Biology, v. 47, no. 4, p. 601–619, accessed April 21, 2020, at https://doi.org/10.1046/j.1365-2427.2002.00916.x.

Heimann, D.C., 2017, Assessment of an in-channel redistribution technique for large woody debris management in Locust Creek, Linn County, Missouri: U.S. Geological Survey Scientific Investigations Report 2017–5120, 25 p., accessed April 19, 2018, at https://doi.org/10.3133/sir20175120.

Johnson, P.A., and Heil, T.M., 1996, Uncertainty in estimating bankfull conditions: Journal of the American Water Resources Association, v. 32, no. 6, p. 1283–1291, accessed July 26, 2018, at https://doi.org/10.1111/j.1752-1688.1996.tb03497.x.

Knighton, D.A., 1998, Fluvial forms and processes—A new perspective: London, Arnold, 383 p.

Leopold, L.B., Wolman, M.G., and Miller, J.P., 1964, Fluvial processes in geomorphology: San Francisco, W.H. Freeman, 522 p.

Lisle, T.E., 1982, Effects of aggradation and degradation on riffle pool morphology in natural gravel channels, northwestern California: Water Resources Research, v. 18, no. 6, p. 1643–1651, accessed August 8, 2018, at https://doi.org/10.1029/WR018i006p01643.

Lisle, T.E., 1987, Using "residual depths" to monitor pool depths independently of discharge: Berkeley, Calif., U.S. Department of Agriculture, Pacific Southwest Forest and Range Experiment Station Research Note PSW–394, 4 p., accessed April 19, 2018, at https://doi.org/10.2737/PSW-RN-394.

Madej, M.A., and Ozaki, V., 1996, Channel response to sediment wave propagation and movement, Redwood Creek, California, USA: Earth Surface Processes and Landforms, v. 21, no. 10, p. 911–927, accessed May 4, 2018, at https://doi.org/10.1002/(SICI)1096-9837(199610)21:10<911::AID-ESP621>3.0.CO;2-1.

Matherne, A.M., Myers, N.C., and McCoy, K.J., 2010, Hydrology of Eagle Creek Basin and effects of groundwater pumping on discharge, 1969–2009: U.S. Geological Survey Scientific Investigations Report 2010–5205, 73 p., accessed August 25, 2017, at https://doi.org/10.3133/sir20105205. [Revised November 2011.]

Montgomery, D.R., Buffington, J.M., Smith, R., Schmidt, K., and Pess, G., 1995, Pool spacing in forest channels: Water Resources Research, v. 31, no. 4, p. 1097–1105, accessed August 8, 2018, at https://doi.org/10.1029/94WR03285.

Nakamura, F., and Swanson, F.J., 1993, Effects of coarse woody debris on morphology and sediment storage of a mountain stream system in western Oregon: Earth Surface Processes and Landforms, v. 18, no. 1, p. 43–61, accessed May 2, 2018, at https://doi.org/10.1002/esp.3290180104.

National Geodetic Survey, 2020, OPUS: Online Positioning User Service: National Geodetic Survey web page, accessed September 9, 2020, at https://geodesy.noaa.gov/OPUS/.

Rydlund, P.H., Jr., and Densmore, B.K., 2012, Methods of practice and guidelines for using survey-grade global navigation satellite systems (GNSS) to establish vertical datum in the United States Geological Survey: U.S. Geological Survey Techniques and Methods, book 11, chap. D1, 102 p. with appendixes, accessed September 7, 2017, at https://doi.org/10.3133/tm11D1.

U.S. Department of Agriculture [USDA] Forest Service, 2015, Final environmental impact statement, North Fork Eagle Creek Wells Special Use Authorization: U.S. Department of Agriculture Forest Service, 574 p., accessed April 19, 2018, at https://www.fs.usda.gov/project/?project=9603.

U.S. Department of Agriculture [USDA] Forest Service, 2016, Record of decision, North Fork Eagle Creek Wells Special Use Authorization: U.S. Department of Agriculture Forest Service, 28 p., accessed July 18, 2018, at https://www.fs.usda.gov/project/?project=9603.

U.S. Department of Agriculture [USDA] Forest Service, Little Bear Fire Burned Area Emergency Response [BAER] Team, 2012, Little Bear Fire burn severity derived from June 18, 2012, Burned Area Reflectance Classifications [BARC]: U.S. Department of Agriculture [USDA] Forest Service online database, accessed March 27, 2020, at https://fsapps.nwcg.gov/afm/baer/download.php?year=2012.

U.S. Geological Survey, 2021a, USGS 08387600 Eagle Creek below South Fork near Alto, NM, *in* USGS water data for the Nation: U.S. Geological Survey National Water Information System database, accessed February 12, 2021, at https://doi.org/10.5066/F7P55KJN. [Site information directly accessible at https://waterdata.usgs.gov/nm/nwis/inventory/?site_no=08387600.]

U.S. Geological Survey, 2021b, USGS 08387550 North Fork Eagle Creek near Alto, NM, *in* USGS water data for the Nation: U.S. Geological Survey National Water Information System database, accessed February 12, 2021, at https://doi.org/10.5066/F7P55KJN. [Site information directly accessible at https://waterdata.usgs.gov/nm/nwis/inventory/?site_no=08387550.]

U.S. Geological Survey, 2021c, USGS 08387575 South Fork Eagle Creek near Alto, NM, *in* USGS water data for the Nation: U.S. Geological Survey National Water Information System database, accessed February 12, 2021, at https://doi.org/10.5066/F7P55KJN. [Site information directly accessible at https://waterdata.usgs.gov/nm/nwis/inventory/?site_no=08387575.]

Wallace, J.B., Webster, J.R., and Meyer, J.L., 1995, Influence of log additions on physical and biotic characteristics of a mountain stream: Canadian Journal of Fisheries and Aquatic Sciences, v. 52, no. 10, p. 2120–2137, accessed May 4, 2018, at https://doi.org/10.1139/f95-805.

**For more information about this publication, contact**
Director, New Mexico Water Science Center
U.S. Geological Survey
6700 Edith Blvd. NE
Albuquerque, NM 87113

For additional information, visit
https://www.usgs.gov/centers/nm-water

Publishing support provided by
Lafayette Publishing Service Center

ISSN 2331-1258 (online)
https://doi.org/10.3133/ofr20221041